

014035

PB 259 185

Publication No. R75-22

Order No. 504

Seismic Design Decision Analysis

Report No. 18

**SEISMIC RISK ANALYSIS FOR
TWO-SITES CASE**

by
WEN-HOW TONG

Supervised by
ROBERT V. Whitman

June 1975

Sponsored by National Science Foundation
Research Applied to National Needs (RANN)
Grants GK-27955 and GI-29936

Additional copies may be obtained from

National Technical Information Service

U.S. Department of Commerce

5285 Port Royal Road

Massachusetts Institute of Technology
Department of Civil Engineering
Constructed Facilities Division
Cambridge, Massachusetts 02139

Report No. 18

SEISMIC RISK ANALYSIS FOR
TWO-SITES CASE

by

Wen-How Tong

Supervised by

Robert V. Whitman

May 1975

Publication No. R75-22

Order No. 504

ABSTRACT

As a first step in analysis of the earthquake safety of lifeline systems, the simplest case of spatially distributed targets is studied: two identical targets in a uniform earthquake source area. The variation of the probability of exceeding a specified level of shaking (at least one of the sites or at both sites simultaneously) with respect to spacing of the targets is analyzed. Both deterministic and probabilistic attenuation laws are considered, and a sensitivity study is performed with respect to the constants of the attenuation law. As part of this study, a more accurate treatment is developed regarding the effect of uncertainty in the attenuation law.

PREFACE

This is the 18th in a series of reports under the general title of Seismic Design Decision Analysis. The overall aim of the research is to develop data and procedures for balancing the increased cost of more resistant construction against the risk of losses during possible future earthquakes. The research has been sponsored by the Earthquake Engineering Program of NSF-RANN under Grant GI-27955X3. A list of previous reports follows this preface.

This report is identical with the thesis submitted by Mr. Tong in partial fulfillment of requirements for the degree of Master of Science. He served as research assistant during the work on this report. Dr. Whitman is Professor of Civil Engineering and is principal investigator for the overall study. Dr. Daniele Veneziano, Assistant Professor of Civil Engineering, and Dr. Ghiath Taleb-Agha, Research Associate, also contributed significantly to supervision of the work.

LIST OF PREVIOUS REPORTS

1. Whitman, R.V., C.A. Cornell, E.H. Vanmarcke, and J.W. Reed, "Methodology and Initial Damage Statistics," Department of Civil Engineering Research Report R74-17, MIT, March 1972.
2. Leslie, S.K. and J.M. Biggs, "Earthquake Code Evolution and the Effect of Seismic Design on the Cost of Buildings," Department of Civil Engineering Research Report R72-20, MIT, May 1972.
3. Anagnostopoulos, S.A., "Non-Linear Dynamic Response and Ductility Requirements of Building Structures Subjected to Earthquakes," Department of Civil Engineering Research Report R72-54, MIT, September 1972.
4. Biggs, J.M. and P.H. Grace, "Seismic Response of Buildings Designed by Code for Different Earthquake Intensities," Department of Civil Engineering Research Report R73-7, MIT, January 1973.
5. Czarnecki, R.M., "Earthquake Damage to Tall Buildings," Department of Civil Engineering Research Report R73-8, MIT, January 1973.
6. Trudeau, P.J., "The Shear Wave Velocity of Boston Blue Clay," Department of Civil Engineering Research Report R73-12, MIT, February 1973.
7. Whitman, R.V., S. Hong, and J.W. Reed, "Damage Statistics for High-Rise Buildings in the Vicinity of the San Fernando Earthquake," Department of Civil Engineering Report R73-25, MIT, April 1973.
8. Whitman, R.V., "Damage Probability Matrices for Prototype Buildings," Department of Civil Engineering Research Report R73-57, MIT, November 1973.
9. Whitman, R.V., J.M. Biggs, J. Brennan III, C.A. Cornell, R. de Neufville, and E.H. Vanmarcke, "Summary of Methodology and Pilot Application," Department of Civil Engineering Research Report R73-58, MIT, October 1973.

10. Whitman, R.V., J.M. Biggs, J. Brennan III, C.A. Cornell, R. de Neufville, and E.H. Vanmarcke, "Methodology and Pilot Application," Department of Civil Engineering Research Report R74-15, July 1974.
11. Cornell, C.A. and H.A. Merz, "A Seismic Risk Analysis of Boston," Department of Civil Engineering Professional Paper P74-2, MIT, April 1974.
12. J.E. Isbell and J.M. Biggs, "Inelastic Design of Building Frames to Resist Earthquakes," Department of Civil Engineering Research Report R74-36, MIT, May 1974.
13. Ackroyd, M.H. and J.M. Biggs, "The Formulation and Experimental Verification of Mathematical Models for Predicting Dynamic Response of Multistory Buildings," Department of Civil Engineering Research Report R74-37, MIT, May 1974.
14. Taleb-Agha, G., "Sensitivity Analyses and Graphical Method for Preliminary Solutions," Department of Civil Engineering Research Report R74-41, MIT, June 1974.
15. Panoussis, G., "Seismic Reliability of Lifeline Networks," Department of Civil Engineering Research Report R74-57, MIT, September 1974.
16. Whitman, R.V., M. Yegian, J. Christian, and Tezian, "Ground Motion Amplification Studies - Bursa, Turkey,"
17. deNeufville, R., "Sensitivity Study Using Utility Functions," Being written.

TABLE OF CONTENTS

	<u>Page</u>
Abstract	1
Preface	2
List of Previous Reports	2
Table of Contents	4
CHAPTER 1 Introduction	7
1.1 Development of Seismic Risk Analysis	7
1.2 Source of Uncertainty in Seismic Risk Analysis	9
1.3 Purpose of the Study	10
CHAPTER 2 Background for Seismic Risk Study	12
2.1 Seismicity	12
2.1.1 Magnitude-Frequency Law	12
2.1.2 Occurrence of Earthquake	16
2.2 Earthquake Source	17
2.3 The Attenuation Law	18
2.4 Example	21
CHAPTER 3 Seismic Risk Study for a Two-Site Case	27

	<u>Page</u>
3.1 Risk Study Using Deterministic Attenuation Law and Deterministic Resistance	28
3.2 Seismic Risk Study for Probabilistic Attenuation Law and Deterministic Resistance	37
3.3 Application	46
3.4 Conclusion	49
References	78
Appendix A Derivation of the Probability of Exceedance for One Point Source and One Site	81
Appendix B List of Figures	85
Appendix C List of Tables	87

Preceding page blank

7

CHAPTER 1. Introduction

1.1 Development of Seismic Risk Analysis

The seismic risk analysis for a specific site was first developed by Cornell⁽⁴⁾. The method combined information about source geometry provided by geologists, time occurrence of earthquakes, seismicity (see Section 2.1) of the region where the site is located and attenuation of ground motion parameters (ground acceleration, velocity, displacement or modified Mercalli Intensity) with respect to magnitude and focal distance provided by seismologists to yield a probabilistic statement about the earthquake threat at a given site. Due to the random nature of earthquake occurrence (time and space) and magnitude of earthquakes, the risk study has to be done in a probabilistic sense. The result of a seismic risk study may be expressed in terms of annual risk, i.e. the probability that a certain level of ground motion will be exceeded annually or may be expressed in terms of "return period" for a given value of ground motion. For example, if a peak acceleration of 0.5 g corresponds to a 100 year return period, then a ground motion with peak ground acceleration greater than or equal to 0.5 g will occur on the average once every 100 years. Another interpretation is that the average annual number of earthquakes causing a peak ground acceleration

greater than or equal to 0.5 g at the site is equal to 0.01. The two above expressions for seismic risk at a site are shown in Figure 1⁽²⁶⁾. The latter expression (i.e. return period) has been used by many authors^(14,18,26,1) in preparing a seismic risk map. A typical risk map is shown in Figure 2⁽²⁶⁾ which shows contours of equal ground motion parameters of a certain return period. Nowadays the seismic risk is most frequently expressed as acceleration (velocity, MMI, etc.) exceeded with x% probability during y year exposure interval. For instance one may state the risk of a structure as follows: there is a 10% probability that the site ground acceleration will exceed a certain level for the 100 year life span of the structure.

Recently, improvements of all kinds have been tried for better fitting experimental data, such as the Markov model of generation of earthquakes⁽²³⁾, the quadratic magnitude-frequency law⁽¹⁹⁾, the general attenuation law⁽⁶⁾, and the Bayesian's approach^(12,17) of risk analysis. Yet all the studies were limited to risk analysis of one specific site. Recently the interest in safety of nuclear power plants generated the study on seismic risk of spatially distributed structures. Spatially distributed structures are not limited only to power plants; they may include a transportation network, an electrical generating and distribution system or a

socioeconomic region or country^(9,21). It is of interest to know what is the risk that Q out of N targets will experience ground motion exceeding certain levels simultaneously annually or within a certain exposure time interval. Two programs were developed to meet this need. The first one was developed in the U.S.S.R. by Keilis-Borok et al^(15,16). It is used to study risk for distributed targets⁽²⁴⁾, line object⁽¹⁵⁾, area object⁽¹⁵⁾ or any combination of these three. The program can be used for circular or elliptical isoseismal models and bent magnitude-frequency law. The second program was developed by Taleb-Agha⁽²⁵⁾. An idea of "Pseudo resistance" was introduced in the analysis to obtain the probability that Q out of N targets fail, where N is the number of targets in the study and Q can be 1,2,3... up to N . It is this second program that the author used for the study which will be presented in Chapter 3.

1.2 Sources of Uncertainty in Seismic Risk Analysis

Besides the randomness of earthquake occurrence, magnitude and focal distance, there are two major sources of uncertainty which may be of importance in the seismic risk analysis. One comes from uncertainty in the attenuation law and the other from the uncertainty in the resistance of the targets. The first kind of uncertainty is due to the complex-

ity of the mechanism of earthquakes, seismic wave propagation, local soil conditions and estimates of seismicity, etc. It has been studied by many authors (7,10,13) and it has been concluded that the natural logarithm of the ratio between observed ground motion parameters and computed ground motion parameters is normally distributed. The second kind of uncertainty (resistance of targets) is due to workmanship of construction, material of structures, etc. Thus it cannot be said that a structure will surely collapse once the site ground motion exceeds a certain level of, say, resistance of the target. It is of interest to know how much these two sources of uncertainty would separately or jointly affect the seismic risk results.

1.3 Purpose of the Study

The study is conducted to investigate the seismic risk of two targets located in a uniform seismic source area. It is of interest to know how the above two uncertainties would affect the risk study. There are four possible combinations of these two kinds of uncertainty in the consideration of seismic risk study. Each combination may yield a different annual risk for the probability that at least one target will fail ("failure" means the event that the site ground acceleration will exceed the resistance) and the probability that two

targets will fail simultaneously. The four combinations are as follows:

<u>Attenuation Law</u>	<u>Structural Resistance</u>
deterministic	deterministic
probabilistic	deterministic
deterministic	probabilistic
probabilistic	probabilistic

However, only first two cases are treated in this thesis, i.e. to study the level at which the consideration of the uncertainty of the attenuation law will affect the results of seismic risk analysis for the two-site case. Finally I will make recommendation as to whether or not to include this uncertainty in the seismic risk analysis.

The thesis is divided into two major parts. The first part considers the case of deterministic attenuation law and deterministic resistance. The variation of risk with respect to spacing between two targets is studied. A sensitivity study is also made in this part. The second part of the thesis studies the treatment of the probabilistic attenuation law in combination with deterministic resistance.

CHAPTER 2

Background for Seismic Risk Study

As mentioned in the last chapter, due to the randomness of earthquake size, time and space distribution of earthquakes, seismic risk study must be treated in a probabilistic manner. Three major random variables in the analysis are the magnitude of the earthquake, the distance from the source to site, and the time occurrence of the earthquake. Each of these will be discussed later.

2.1 Seismicity

2.1.1 Magnitude-frequency law

The seismicity of a region can be considered as the relationship between the number of occurrences of earthquakes and their magnitudes in a given time for that region. This relation is usually expressed as in Richter's Law,

$$\log_{10} N(m) = a - bm \quad (1)$$

where a and b are regional constants and m is earthquake magnitude expressed in the Richter scale, usually ranging between 3 and 8.7. From equation 1 follows

$$N(m) = 10^a e^{-\beta m} \quad (2)$$

where $N(m)$ gives the mean number of earthquakes with magnitude greater than m occurring within a unit time, and β is equal to $b \cdot \ln 10$. The β value is quite stable from region to region; for instance β is 1.65 for the Boston area, 1.38 for the eastern United States and 2.02 for the whole United States. (8) Usually in the engineering risk analysis a lower bound m_0 is set for earthquake magnitude. Any earthquake with magnitude smaller than m_0 is not of engineering interest. Thus $N(m_0)$ gives the total number of earthquakes which are of engineering interest within a unit time. Then the ratio of $N(m)$ to $N(m_0)$ gives the probability that earthquake magnitude will be greater than or equal to m , i.e.,

$$G_M(m) = P[M \geq m] = 1 - F_M(m) = \frac{N(m)}{N(m_0)} = e^{-\beta(m-m_0)} \quad m \geq m_0 \quad (3)$$

where $G_M(m)$ is the complementary cumulative distribution function of earthquake magnitude. If we try to express the size of the earthquake in terms of epicentral intensity, then a relation between magnitude and epicentral intensity must be

adopted. Here an empirical form suggested by Richter⁽²²⁾ is adopted:

$$M = 1 + \frac{2}{3} I_0 \quad (4)$$

where I_0 is the epicentral intensity. Then the complementary cumulative distribution function of epicentral intensity can be expressed as

$$G_{I_0}(i) = P[I_0 > i] = 1 - F_{I_0}(i) = e^{-\frac{2}{3}\beta(i-i_0)} \quad i \geq i_0 \quad (5)$$

where $G_{I_0}(i)$ is the complementary cumulative distribution function and i_0 is the lower bound of epicentral intensity.

From equations (4) and (5) we see that β values for magnitude and epicentral intensity are different. A table of conversion for β is shown below⁽²⁷⁾.

Table 1. Conversion Table of β

from	D	F	H	J
to				
D	1	$\ln 10$	$2/3$	$(2/3) \ln 10$
F	$\log e$	1	$(2/3) \log e$	$2/3$
H	$3/2$	$(3/2) \ln 10$	1	$\ln 10$
J	$(3/2) \log e$	$3/2$	$\log e$	1

where

$$\ln N[I_0 > i_0] = C - DI_0$$

$$\log N[I > i_0] = E - FI_0$$

$$\ln N[M > m] = G - HM$$

$$\log N[M > m] = I - JM$$

$$\text{and } M = \frac{2}{3} I + 1$$

The values for a and b in equation (1) have been studied for several regions in the world and for the whole earth⁽²⁾. The plot of equation (1) is shown in Figure 3. An implication from the plot for the whole earth is that there is an upper bound for earthquake magnitudes. Since Richter's law for very large magnitudes implies an infinite energy released by earthquakes, Cornell and Vanmarcke⁽⁵⁾ proposed a modified magnitude-frequency relation considering the existence of an upper bound of magnitude.

$$F_M(m) = k_{m_1} (1 - e^{-\beta(m-m_0)}) \quad m_0 \leq m \leq m_1 \quad (6)$$

where $k_{m_1} = (1 - e^{-\beta(m_1-m_0)})^{-1}$ is a mandatory factor needed to normalize the cumulative distribution function to unity at m equal to m_1 , the maximum possible value of magnitude based on the geological and seismological data of the region.

The suggestion to use a quadratic magnitude-frequency law instead of a linear one is based on the fact that the

quadratic form fits well the observed cumulative distribution function of magnitude as shown in Figure 4⁽¹⁹⁾. Also shown in the figure is a plot for the linear untruncated form. It can be seen that this linear untruncated form overestimates the occurrence of large events. As for the linear truncated form, the sharp discontinuity at the upper bound m_1 does not reflect the true state. However, the use of linear magnitude-frequency law yields a more conservative risk result than does the quadratic form. In this study a linear truncated form is used. For details about quadratic magnitude-frequency law, see reference 19.

2.1.2 Occurrence of Earthquakes

Generally the number of earthquake occurrences in the future is a random variable and this randomness of occurrence has to be incorporated into the seismic risk study. It is assumed that these events, with magnitude greater than or equal to m_0 , follow a Poisson process with average rate of occurrence ν per year. Then the probability distribution of \hat{N} , the number of earthquakes of engineering interest ($m \geq m_0$)⁽³⁾ is

$$p_{\hat{N}}(n) = \frac{e^{-\nu t} (\nu t)^n}{n!} \quad n=0,1,2,\dots \quad (7)$$

Among these major earthquakes only those which cause site ground motion exceeding y will make contributions to the seismic risk study. These special events also follow a Poisson process with average rate of occurrence $P_y v$, where P_y is the probability that site ground motion exceeds y given an earthquake occurs, as will be shown in Section 2.4. Thus the probability distribution of N , the number of earthquakes that site ground motion will exceed y in a time interval t is⁽⁴⁾

$$P_N(n) = \frac{e^{-P_y v t} (P_y v t)^n}{n!} \quad n=0,1,2,3 \quad (8)$$

2.2 Earthquake Source

In the seismic risk study for either a specific site or spatially distributed sites, the suspected earthquake source must be identified. Usually the source may be represented as a point source, line source (fault) or area source. The point source is the simplest and most basic case in the risk study. The area source is used when the occurrence of earthquakes in a particular region is not associated with a surface fault and/or insufficient data are available. Cornell⁽⁵⁾ pointed out that if the source is about two times the focal distance away from the site, then the exact shape of the source is not really of much importance. In this study a uniform source

area is assumed. Here "uniform" means the same rate of occurrence per unit area, the same focal depth, the same attenuation everywhere. Due to the fact that the major contribution of seismic risk is from the more frequent, smaller and closer earthquake sources⁽⁵⁾, a circular bounded source area may be defined for each site. We call this area the circular source area of influence. Any earthquake occurring outside this circular area will not produce a site ground motion exceeding a certain level. The radius of this circular area is determined from incorporating the attenuation law, the upper bound of magnitude in that region, and the resistance of the target, as will be shown later.

2.3 Attenuation Law

Once an earthquake occurs the ground motion will propagate and attenuate with respect to distance away from the epicenter. The rate of attenuation depends on the condition of the ground. For firm ground the earthquake wave attenuates faster. The attenuation law is a functional empirical formula relating the site ground motion parameters (acceleration, velocity, displacement or MMI) to earthquake magnitude and distance between epicenter and the site. Oliveira⁽²⁰⁾ compiled the attenuation laws proposed by different authors. The most common one is that suggested by Esteva⁽¹¹⁾.

$$Y = b_1 e^{b_2 M} R^{-b_3} \quad (9)$$

where b_1 , b_2 , b_3 are attenuation constants subjected to estimation over a broad region; Y may be acceleration (cm/sec²), velocity (cm/sec), or displacement (cm); M is the earthquake magnitude expressed in Richter's scale; and R is the focal distance expressed in kilometers. Esteva⁽¹³⁾ suggested an empirical modification to the above attenuation law in order to get a better fit for the recorded data.

$$Y = b_1 e^{b_2 M} (R + 25)^{-b_3} \quad (10)$$

This constant is added to control the ground acceleration for a small focal distance. As shown in Figure 5⁽¹⁰⁾, the least square fits using the two above attenuation laws (equation 9 and 10) for recorded data of the 1971 San Fernando Earthquake. The one using equation 10 gives a better fit.

For some areas, such as the eastern United States, because of a lack of recorded data, the ground motion parameter was described by modified Mercalli intensity. In this case the attenuation of earthquake motion is expressed in terms of MMI⁽⁸⁾.

$$I_{\text{site}} = I_{\text{epicenter}} \quad R < 10 \text{ Miles} \quad (11)$$

$$I_{\text{site}} = C_1 + C_2 I_{\text{epicenter}} - C_3 \ln R$$

$R < 10 \text{ miles}$

In using this attenuation law, attention must be paid to use the correct β value.

The risk analysis is very sensitive to the attenuation constant b_3 (or c_3), as will be shown in a later section. When the epicenter is close to the site, the value of the focal depth becomes very important. As Cornell pointed out, the seismic risk for one site is contributed to mainly by those smaller earthquakes and closer sources. That is why the risk analysis is sensitive to focal depth. In this thesis, the study is oriented to comparison between the risk of one and two sites, so the best estimation of focal depth is not critical. It has been found that there is an important dispersion between the observed ground motion and the predicted one by using the attenuation law in equation (10). This brought up the study of probabilistic attenuation law^(6,13). The influence of using probabilistic attenuation law in risk analysis will be dealt with later.

2.4 Example

In order to illustrate the seismic risk analysis which combines the above information, an example of one target located in a uniform source area will be investigated. Here "uniform" means that everywhere in this area, the upper and lower bounds of magnitude, the rate of occurrence of earthquakes, and the constants in the attenuation law are the same. As mentioned earlier in Section 2.1.1, the maximum magnitude of an earthquake is finite, say m_1 . Usually this value varies from 8.3 to 8.7, depending on the tectonics of the region under consideration. Then in combination with attenuation of earthquake waves and structural resistance y , a focal distance r_y can be defined. Any earthquake occurring outside this range will not cause site ground motion exceeding level y . The effect of limiting study to earthquake sources within r_y is to eliminate part of the source or sources which are located beyond r_y . The seismic risk result having an upper bound m_1 is different from the risk having no upper bound, depending both upon m_1 and upon y .

As a first step in the analysis, a source area must be defined within this uniform source area by utilizing the attenuation law, upper bound m_1 and resistance y . Here

equation (9) is used for attenuation law. The 25 km modification factor could be easily incorporated, if necessary. By defining attenuation law as

$$Y = b_1 e^{b_2 M} R^{-b_3}$$

and setting upper bound m_1 , resistance y ,

$$r_y = \left(\frac{y}{b_1}\right)^{-\frac{1}{b_3}} e^{\frac{b_2 m_1}{b_3}} \quad (12)$$

Figure 6 shows the picture clearly. Suppose a point source i is at a distance r away from the site and at an angle θ from the $x-x$ axis (as shown in figure 6). The probability that site ground motion will exceed level y given an earthquake occurring at this point is:

$$\begin{aligned} P[Y \geq y | (r, \theta)] &= P[b_1 e^{b_2 M} r^{-b_3} \geq y | (r, \theta)] \\ &= P[M \geq \frac{1}{b_2} \ln \frac{y r^{b_3}}{b_1} | (r, \theta)] \end{aligned} \quad (13)$$

For the limited magnitude-frequency distribution

$$F_M(m) = K_{m_1} [1 - e^{-\beta(m-m_0)}] \quad m_0 \leq m \leq m_1 \quad (6)$$

Combining equation (6) and (13)

$$\begin{aligned}
 P[Y > \underline{y} | (r, \theta)] &= P[M > \frac{1}{-b_2} \ln \frac{yr}{b_1} | (r, \theta)] \\
 &= 1 - F_M\left(\frac{1}{b_2} \ln \frac{yr}{b_1}\right) \\
 &= 1 - K_{m_1} [1 - e^{-\beta\left(\frac{1}{b_2} \ln \frac{yr}{b_1} - m_0\right)}]
 \end{aligned}$$

$$y' \leq y \leq y''$$

$$\text{where } y' = b_1 e^{b_2 m_0} r^{-b_3}$$

$$y'' = b_1 e^{b_2 m_1} r^{-b_3}$$

$$\therefore P[Y > \underline{y} | (r, \theta)] = 1 - K_{m_1} [1 - e^{\beta m_0} (y/b_1)^{-\beta/b_2} r^{-b_3 \beta/b_2}] \quad (14)$$

if $m_1 = \infty$, then

$$P[Y > \underline{y} | (r, \theta)] = e^{\beta m_0} r^{\frac{b_3 \beta}{b_2}} \left(\frac{y}{b_1}\right)^{\frac{-b_3 \beta}{b_2}} \quad (14a)$$

From figure 6 we see that this circular source area of influence is defined by a focal distance r_y or a horizontal distance $\sqrt{r_y^2 - d_0^2}$. If we assume that within this circular source area any point is equally likely to have an earthquake occur, then

the probability that an earthquake will occur at point i (r, θ) is just the ratio of the area of point source i to the circular source area, i.e.

$$\begin{aligned} P[\text{an earthquake occurs at } i] &= \frac{(\rho d\theta) d\rho}{\pi(r_y^2 - d_0^2)} \\ &= \frac{\int_{r_0}^{r_y} \left(\frac{1}{2} \frac{2r}{\sqrt{r^2 - d_0^2}}\right) dr d\theta}{\pi(r_y^2 - d_0^2)} = \frac{r dr d\theta}{\pi(r_y^2 - d_0^2)} \quad (15) \end{aligned}$$

where $d_0 \leq r \leq r_y$ and $0 \leq \theta \leq 2\pi$.

$$\begin{aligned} \therefore p_y = P\{Y \geq y\} &= \int_{d_0}^{r_y} \int_0^{2\pi} P\{Y \geq y | (r, \theta)\} \frac{r}{\pi(r_y^2 - d_0^2)} dr d\theta \\ &= \int_{d_0}^{r_y} dr \int_0^{2\pi} \left\{ 1 - k_{m_1} \left[1 - e^{\beta m_0} \left(\frac{y}{b_1}\right)^{-\beta/b_2} r^{-\frac{b_3 \beta}{b_2}} \right] \right\} \frac{r}{\pi(r_y^2 - d_0^2)} d\theta \\ &= \frac{2}{r_y^2 - d_0^2} \int_{d_0}^{r_y} \left[r(1 - k_{m_1}) + k_{m_1} e^{\beta m_0} \left(\frac{y}{b_1}\right)^{-\beta/b_2} r^{-\frac{b_3 \beta}{b_2} + 1} \right] dr \\ &= (1 - k_{m_1}) + \frac{2}{r_y^2 - d_0^2} k_{m_1} e^{\beta m_0} b_1^{\beta/b_2} \left[\frac{d_0^{-\frac{b_3 \beta}{b_2} + 2} \left(1 - (r_y/d_0)^{-\frac{b_3 \beta}{b_2} + 2} \right)}{\frac{b_3 \beta}{b_2} - 2} \right] y^{-\beta/b_2} \quad (16) \end{aligned}$$

We can see now that the risk p_y here is independent of the θ angle extended by the source. In the above expression $\frac{2}{r_y^2 - d_o^2} \left\{ \frac{d_o^{-\frac{b_3}{b_2}\beta+2} (1 - (r_y/d_o)^{-\frac{b_3}{b_2}\beta+2})}{b_3\beta/b_2 - 2} \right\}$ is a geometric term. Cornell and Vanmarcke⁽⁵⁾ have graphed this geometric term for point source, line source and for area source. Such graphs greatly ease the integration for the geometric term. In general the source area or line source is discretized into a number of point sources. The risk contributed from each point source is studied and finally all the contributions are summed up. This strategy has its advantages when the computer is utilized.

The above discussion gives only the probability that the site ground motion will exceed a certain level y . Now we should consider the time occurrence of the earthquake. By assuming that the earthquake occurs with magnitude greater or equal to m_o as a Poisson process, then

$$P_{\hat{N}}(n) = \frac{e^{-vt} (vt)^n}{n!} \quad (7)$$

where $v = (\text{number of earthquakes per year per unit area}) \times (\text{circular area})$. Among these earthquakes which occur within one year we are only interested in those events which cause site ground motion exceeding y , with the rate of occurrence of these earthquakes equal to $p_y \cdot v$. A property of the Poisson process is that the event having rate of occurrence $p_y v$ is

still a Poisson process⁽¹³⁾. Thus,

$$P_N(n) = \frac{e^{-p_Y v t} (p_Y v t)^n}{n!} \quad (8)$$

$\therefore P[Y_{\max} < y] = P[\text{no events will exceed } y]$

$$= P[N=0] = e^{-p_Y v t}$$

$$P[Y_{\max} > y] = 1 - e^{-p_Y v t} \quad (17)$$

From equation (17) one can assess the risk of a structure as acceleration exceeded with $1 - e^{-p_Y v t_0}$ probability during an exposure interval of t_0 years. One can also find annual risk by

$$P[Y_{\max} > y] = 1 - F_{Y_{\max}}(y) = 1 - e^{-p_Y v} \quad (18)$$

If $p_Y v$ is small, then the annual risk is approximately equal to $p_Y v$. The average annual return period T of ground motion level y equals the reciprocal of the probability that the annual Y_{\max} exceeds y , i.e.

$$T = \frac{1}{P[Y_{\max} > y]} \approx \frac{1}{p_Y v} \quad \text{if the risk is low.}$$

CHAPTER 3

Seismic Risk Study for a Two Site Case

In this chapter the risk study for two sites located in a uniform source area is conducted for: (a) deterministic attenuation law and deterministic resistance and (b) probabilistic attenuation law and deterministic resistance. The first development of engineering seismic risk analysis gave only the risk of a specific site. In later developments the probabilistic attenuation law was still limited to the one site problem⁽⁷⁾. Recently Taleb-Agha used a concept of "pseudo resistance"⁽²⁵⁾ to study the risk to spatially distributed targets. This scheme enables one to find the probability of Q out of N targets failing. The model of the earthquake source could be either a line source or a source area. In Section 3.2 the study focused on the probabilistic attenuation law. The effect of taking into account the uncertainty of the attenuation law in the risk study is to increase the risk (for a given design resistance). The magnitude of this effect depends on the standard deviation of this uncertainty term and other factors.

3.1 Risk Study Using Deterministic Attenuation Law and Deterministic Resistance

The most important idea used in studying the seismic risk to a system of spatially distributed targets is "pseudo resistance⁽²⁵⁾". This treatment is based on the study of a point source. Thus, either a linear source or a source area must first of all be discretized. For a point source and a system of spatially distributed targets, the pseudo resistance for each target is defined as follows:

$$\bar{R}_i = y_i r_i^{b_3} \quad (20)$$

where y_i is the resistance of the i th target expressed in cm/sec^2 , r_i is the focal distance (in Kilometers) between the i th target and the point source and b_3 is the attenuation constant for the region under consideration. By doing so the problem is then modeled by a system of targets on a circle of one kilometer radius surrounding the point source. Each target has its own pseudo resistance defined by $y r^{b_3}$. This concept is shown in Figure 7⁽²⁵⁾. All pseudo resistances are then arranged in the order of increasing magnitude:

$$\bar{R}_1 < \bar{R}_2 < \dots < \bar{R}_n \quad (21)$$

Thus, if an earthquake occurs at the point source, the probability that Q or more out of N targets will experience ground motion exceeding a certain level \bar{R}_q simultaneously can be found as follows:

$P[Q \text{ or more out of } N \text{ targets fail} | \text{an earthquake occurs}] =$

$$P[Y \geq \bar{R}_q | \text{an earthquake occurs}] = P[M_i \geq \frac{1}{b_2} \ln \frac{\bar{R}_q}{b_1} | \text{earthquake occurs}] \quad (22)$$

where M_i is the earthquake magnitude for point source i . The probability of exactly Q out of N failing is then given by:

$$P[\text{exactly } Q \text{ out of } N \text{ failing}] = P[Q \text{ or more out of } N \text{ fail} | \text{an earthquake occurs}] - P[(Q+1) \text{ or more out of } N \text{ fail} | \text{an earthquake occurs}]$$

As mentioned earlier, this scheme is limited to a point source. For a source area, the area has to be discretized into point sources. In this program the discretization is carried out by using triangular element. Each triangular element (area ΔA_i) is then modeled by a point source at the center of gravity of the triangular element. Here we assume that it is equally likely for an earthquake to occur at any point within this source area. The probability density function of occurrence is then defined as $1 / \text{Total area of the source}$. Thus the probability of Q or more out of N targets failing, given the source area, is:

$$P_f = P[Q \text{ or more out of } N \text{ targets failing}] = \sum_{i=1}^{EQ} P[M_i \geq \frac{1}{b_2} \ln \frac{\bar{R}_q}{b_1} | \text{an earthquake occurs at } i] f_{xy}(x_i, y_i) \Delta A_i \quad (23)$$

where " $f_{xy}(x_i, y_i)$ " is the probability density function of occurrence for point source i and is equal to

$$\frac{1}{\text{total area of source}}$$

" ΔA_i " is the element area of point source i

"EQ" is the total number of point sources within the discretized source area.

If we assume that the occurrence of major earthquakes (i.e. $M > m_0$) follows a Poisson process then the probability of Q or more out of N failing within a time period t is:

$$P[Q \text{ or more out of } N \text{ failing within } t] = 1 - e^{-\nu P_f t} \approx \nu P_f t \quad \text{for low risk} \quad (24)$$

where ν is the mean rate of occurrence of the earthquakes with magnitude greater than m_0 for a given source area within a unit time.

Based on the above reasoning, a study was made for the two-site problem to investigate the change of the seismic risk with respect to the spacing between the two sites. Later a sensitivity study was made to investigate the influence of those parameters which were used in the seismic risk study. In the study done in this thesis a uniform source area was assumed and was modeled by a circular area of influence defined by using the attenuation law and maximum earthquake magnitude of that source area as was done in

Section 2.4. For each of the two sites a separate circular area of influence is found as shown in Figure 8. Any earthquake occurring outside this region cannot cause the site ground motion to exceed a certain level y . Only those earthquakes which occur within the intersected area (1-2-3-4) can possibly cause the two sites to fail simultaneously depending on the magnitude generated by an earthquake. This concept provides a quick check on whether both targets will fail simultaneously as will be shown later in a more general case. In this study the same resistances are assumed for both targets.

To prepare the input data, the above source area of influence can be approximated in the following two ways. The more accurate but more tedious way is to approximate the area by a polygon. The second one and more time-saving way is to approximate the source area by a circumscribing rectangle (as shown in Figure 8). The effects of using a bigger rectangular source area are: (1) an increase in the rate of occurrence for this rectangular area; (2) a decrease in the probability density function of occurrence. However, these two effects cancel each other. It was observed that the risks obtained using these two approximations to model the source area are the same.

For a given set of information about seismicity, attenuation law, resistance, etc., the seismic risk results were plotted from the computer output, Figures 9,10,11. As shown in Figure 9, when the spacing between two sites increases, the probability of at least one site failing also increases. This increase is due to the increase of potential source area. But on the other hand the probability that two sites fail simultaneously decreases due to the decrease of intersected area as spacing increases. When the two sites are so far apart that the two circular areas are tangent to each other, then:

$$\begin{aligned}
 P[\text{at least one fails}] &= P[A \text{ fails} \cup B \text{ fails}] \\
 &= P[A \text{ fails}] + P[B \text{ fails}] - P[A \cap B \text{ fail}] \\
 &= P[A \text{ fails}] + P[B \text{ fails}] \\
 &= 2P[A \text{ fails}] = 2P[\text{two fail as} \\
 &\qquad\qquad\qquad \text{spacing equals to} \\
 &\qquad\qquad\qquad \text{zero}] \qquad\qquad (25)
 \end{aligned}$$

This can be seen at point I in Figure 9. At this stage the failure events of A and B are independent of each other. Any earthquake occurrence will influence only one site (either A or B), and nothing more. The probability that the two sites will fail simultaneously at this spacing becomes zero as shown in Figure 11.

From the above results we can learn that once the maximum epicentral magnitude of a region and the attenuation law are known, a circular radius ($\sqrt{r_y^2 - d_0^2}$) can be found as discussed above and when the spacing between two sites is two times this radius, there is no risk of these two targets failing at the same time. This reasoning can be applied in a more general sense to provide a quick check for the problem involving spatially distributed sites. For example, take the case of a three-site system located in two different uniform source areas, as shown in Figure 12. One can draw a circular area of influence for each of the three sites. Because the seismicities in source area I and source area II are different, some of the source areas of influence are no longer bounded simply by a circle. As shown in Figure 12, the dashed and dotted circular arcs define the area of influence for site 3, the solid line circular arcs define the area of influence for site 2, and the dashed circular arcs define the area of influence for site 1. One can tell quickly from this figure that any earthquake occurring in A_1 will have the possibility of causing the three sites to fail simultaneously and that any earthquake occurring in A_2 or A_3 will have the possibility of causing two sites to fail simultaneously.

The seismic risk results for the two site case are presented in a set of normalized curves in Figure 13. The

ordinate is $P[\text{two fail simultaneously}]/P[\text{single site fails}]$ and the abscissa is spacing/radius of circular area. This radius of circular area ($\sqrt{r_y^2 - d_o^2}$) is determined by the attenuation law, structure resistance and upper bound of magnitude as mentioned above. Shown in Figure 13 is a set of curves for $\beta = 1.65$, $b_1=1100$, $b_2=0.5$, $b_3=1.32$, resistance=100 cm/sec² and $m_1=6.0$ to 8.3. From this kind of curve one can determine how much the spacing should be in order for the probability of two sites failing simultaneously to be equal to a certain percentage (say 1%, 5%, etc.) of the probability of two sites failing simultaneously at a spacing of zero (i.e. probability of a single site failing).

Three different attenuation laws suggested by Esteva⁽¹³⁾ and Donovan⁽¹⁰⁾ were used in the risk study for the two site case. They are:

$$\text{Esteva} \quad a = 1260 e^{0.8M} (R+25)^{-2.0} \quad (26)$$

$$\text{Donovan} \quad a = 1350 e^{0.58M} (R+25)^{-1.52} \quad (27)$$

$$\text{Donovan} \quad a = 1100 e^{0.5M} (R+25)^{-1.32} \quad (28)$$

where a is the ground acceleration (cm/sec²), M is the earthquake magnitude (Richter scale) and R is the focal distance (Kilometers). The seismic risk results obtained by using these three different attenuation laws are plotted in Figures 14 and 15 for the event of at least one site failing

and for the event of two sites failing simultaneously. In Figure 16 the results obtained by using the different attenuation laws are normalized as was done for Figure 13. As can be seen in Figures 14 and 15, all three results are different. The result in which Esteva's attenuation law is used gives the lowest risk. A sensitivity study was then made in order to determine which attenuation law constants are more important in the seismic risk analysis of a two-site system. In this sensitivity study b_1 was changed from 1100 to 1350, b_2 was changed from 0.5 to 0.58 and b_3 was changed from 1.32 to 1.52. Seismic risk results using these different constants are plotted in Figures 17 and 18 for the events of one site failing and two sites failing, respectively. Figure 19 shows the set of normalized curves of this study. The results show that the risk for both events are very sensitive to b_2 and b_3 . Small differences in the estimation of b_2 or b_3 for the region under study could cause a significant difference in the result of seismic risk. However, as shown in the graphs the risk is less sensitive to b_1 . When the value of b_3 is relatively large, the main contribution to the risk is from closer sources, i.e. the circular area of influence is small. Thus, in this case the estimation of focal depth is very important, because the focal distance is greatly influenced by the value of the

focal depth when the sources are close to the site.

3.2 Seismic Risk Study for Probabilistic Attenuation Law and Deterministic Resistance

In Sec. 3.1, the risk analysis accounts for the uncertainty in the magnitude of the earthquake, for the uncertainty of the earthquake location and the distance between the site and the source, and for the randomness in the rate of the earthquake occurrences. A deterministic attenuation law was used in Sec. 3.1. This deterministic attenuation law is assumed as a functional relationship between the site ground motion parameter on one hand and the earthquake magnitude and distance on the other hand. In fact, there is only a crude correlation between the variables. There is a significant scatter of the observed data about the values predicted by using this deterministic attenuation law. This dispersion is due to the fact that the deterministic attenuation law does not account for the complexity of the mechanism of the earthquakes, for the seismic wave propagation and for the local soil condition etc. The uncertainty due to these factors will be represented by a random variable in the treatment of the risk study, as it is important to study the influence of this uncertainty in the seismic risk analysis.

Esteva⁽¹²⁾ has found that the residuals about a least

square fits to $\ln Y$ (the natural logarithm of the predicted ground motion parameter) are approximately normally distributed. This implies that the uncertainties due to the factors mentioned above are contributed in a multiplicative manner. Thus the deterministic attenuation law can be replaced by one containing an additional term (i.e. the probabilistic attenuation law). In this probabilistic attenuation law the following relationship among the ground motion parameter Y , the earthquake magnitude M and the distance R applies:

$$Y = b_1 e^{b_2 M} R^{-b_3} \varepsilon \quad (29)$$

where the natural logarithm of ε is normally distributed with mean zero and a standard deviation σ (of the order of 0.5 to 1.0)⁽⁷⁾. However a value of σ as low as 0.2 has been used by Cornell⁽⁸⁾. Because of the presence of this additional random variable ($\ln \varepsilon$), one has to integrate over all possible values of $\ln \varepsilon$ ($-\infty$ to $+\infty$) in the risk study. As will be shown, the effect of including this uncertainty term in the risk study is an increase in the seismic risk analysis for a given resistance. Thus, the design level of the resistance has to be raised in order to maintain a given risk.

As mentioned before, in automated computation it is easier and more versatile for the risk analysis to first

reduce the source area into discrete point sources. Then, each point source is treated independently and finally all the contributions are summed. Thus, in the study of a seismic risk which takes the uncertainty term in the attenuation law into account, we still use point sources as the base of study. The advantage of doing this will be seen later. For a point source (i.e. with a fixed focal distance) having an exponential magnitude distribution with an upper bound m_1 and a lower bound m_0 , the probability that the ground motion Y will exceed the resistance y , given that an earthquake occurs, is shown as follows (for derivation, see Appendix A):

$$P\{Y \geq y | \text{an earthquake occurs}\} = k_{m_1} \Phi^*\left(\frac{Z_2}{\sigma}\right) + (1 - k_{m_1}) \Phi^*\left(\frac{Z_1}{\sigma}\right) + k_{m_1} \left[\Phi^*\left(\frac{Z_1}{\sigma} - \frac{\beta \sigma}{b_2}\right) - \Phi^*\left(\frac{Z_2}{\sigma} - \frac{\beta \sigma}{b_2}\right) \right] e^{\frac{\beta^2 \sigma^2}{2 b_2^2}} e^{\beta m_0} R^{-\frac{b_3 \beta}{b_2} \left(\frac{y}{b_1}\right)^{-\frac{\beta}{b_2}}} \quad (30)$$

where $k_{m_1} = (1 - e^{-\beta(m_1 - m_0)})^{-1}$ is a normalizing factor

$\Phi^*(\cdot)$ is the complementary cumulative distribution

function of a standardized Gaussian distribution.

$$Z_1 = \ln y - \ln(b_1 e^{b_2 m_1} r^{-b_3})$$

$$Z_2 = \ln y - \ln(b_1 e^{b_3 m_0} r^{-b_3})$$

Next, we shall study the effect which the inclusion of the uncertainty in the attenuation law has on the risk result. First we will consider the case where there is no upper bound

on the earthquake magnitude, i.e. $m_1 = \infty$ and $k_{m1} = 1$. Then, the probability of equalling or exceeding y can be simplified to:

$$P\{Y \geq \text{an earthquake occurs}\} = \Phi^*\left(\frac{Z_2}{\sigma}\right) + \left[1 - \Phi^*\left(\frac{Z_2}{\sigma} - \frac{\beta\sigma}{b_2}\right)\right] \times e^{\frac{\beta^2\sigma^2}{2b_2^2}} e^{\beta m_0} r^{-\frac{b_2\beta}{b_1}\left(\frac{y}{b_1}\right) - \frac{\beta}{b_2}} \quad (31)$$

By comparison with Equation (14a) one can see that $e^{\beta m_0} r^{-\frac{b_2\beta}{b_1}\left(\frac{y}{b_1}\right) - \frac{\beta}{b_2}}$ is just the probability of equalling or exceeding y when the uncertainty in the attenuation law is not taken into account in the analysis. The $e^{\frac{\beta^2\sigma^2}{2b_2^2}}$ term is a penalty term for the uncertainty and the $\Phi^*(\cdot)$ functions taken into account the effect of the level of the resistance relative to m_0 . Two examples of the point source case are studied and the results are presented in Figures 20 and 21. Several remarks can be made regarding these studies:

1. If the resistance is high relative to m_0 , the $\frac{Z_2}{\sigma}$ terms in Equation (31) can be neglected without causing any significant change in the results. Neglecting the $\frac{Z_2}{\sigma}$ terms, the effect of including the attenuation law uncertainty in the study is to give a risk which differs from the seismic risk result obtained by using the deterministic attenuation law by a factor of $e^{\frac{\beta^2\sigma^2}{2b_2^2}}$ as shown in Fig. 20.
2. If the resistance is low and the focal distance is

such that $\frac{1}{b_2} \ln \frac{R^{b_3} y}{b_1}$ is close to m_0 , then the effect of using the probabilistic attenuation law is negligible and the ratio of the risk due to the probabilistic attenuation law to that due to the deterministic attenuation law is roughly equal to 1, as shown in Fig.21. The deterministic attenuation law is applicable for those cases where y is equal to or greater than y_{min} ($y_{min} = b_1 e^{b_2 m_0} r^{-b_3}$). When the resistance y is equal to or smaller than y_{min} the probability of equaling or exceeding y is equal to 1. However, the probabilistic attenuation law does not have this limitation. As the resistance y further decreases from y_{min} , the probability of equalling or exceeding y increases and eventually reaches unity. This is the reason why the probabilistic risk curve in Fig. 21 bends as the resistance is getting smaller.

3. From the above discussion a conclusion can be made: ignoring the $\frac{Z_2}{\sigma}$ terms in Equation(31) in the risk analysis gives a conservative result. The upper limit of the effect of using the probabilistic attenuation law is $e^{\frac{\beta^2 \sigma^2}{2 b_2^2}}$.

If the truncated magnitude distribution is considered

in the study, Equation(30) should be applied to find the probability of equalling or exceeding y . Again an example is studied and, as expected, the effect of using the probabilistic attenuation law is an increase in the risk for a given design resistance(as shown in Figure 22). For most of the range of the resistance the $e^{\frac{\beta^2 \sigma^2}{2\mu^2}}$ factor is still a good and conservative approximation for the effect, as long as m_1 and m_0 are not close together (e.g. $m_1 - m_0 \geq 3$). In this truncated case, the effect depends highly on the level of resistance relative to both m_1 and m_0 . This can be seen in Fig.22. The difference between the two results is very great near the upper bound(dotted line). However, it would be overconservative and unrealistic to make any conclusion from this part of the result, where the risk result obtained by using the probabilistic attenuation law is 20 or 30 or even more times that obtained by using the deterministic attenuation law.

The above discussion on the probabilistic attenuation law was focused on the case of one fixed point source and one site. This point source study enables the computer program used in Sect.3.1 to treat the uncertainty in the attenuation law for a spatially distributed system located in a uniform

source area by simply modifying a subroutine. Because there is an extra term ϵ in the attenuation law, the determination of the circular source area of influence can no longer consider the earthquake magnitude and the resistance alone. The effect of ϵ must be included. The following equation applies here:

$$r_y = \left(\frac{b_1}{y} e^{b_2 m_1} \epsilon \right)^{\frac{1}{b_3}} \quad (32)$$

As can be seen in Eq.(32), the r_y depends on ϵ . However, it is found that one has only to consider those sources bounded by the circle whose radius is determined by using $\epsilon = e^{n\sigma}$ in Eq.(32), where n is a finite value and depends on the value of σ and the resistance. Any source outside this $\sqrt{r_y^2 - d_0^2}$ boundary does not contribute significantly to the site risk. As can be seen from Tables 2,3,4,5,6, and 7 this n value depends on σ and on the site resistance. When σ is very small (e.g. 0.02) one can get the same risk results in spite of whether $n=1,2,3, or 4 is used to determine the circular source area of influence. It is also consistent that the seismic risk obtained by using the probabilistic attenuation law with a small σ is essentially the same as the risk obtained by using the deterministic attenuation law. For large value of σ (e.g. 0.5~0.7) or higher resistance$

(e.g. 300cm/sec^2) a large value of n (e.g. 2-5) has to be used in order to take into account the effect of ϵ .

The procedures for the analysis can be stated as follows:

1. Discretize the source area into i point sources.
2. For each of the i point sources calculate $[1-F_y(y)]$ using either Eq. (30) or (31), depending on the type of magnitude distribution used.
3. Sum up the $[1-F_y(y)]$ of all discretized point sources within the source area.
4. For this specific source area, the risk that in the time period t the maximum peak ground motion parameter at the site will exceed y is:

$$P(Y_{\max} \geq y) = 1 - \exp[-\gamma t(1-F_y(y))] \approx \gamma t(1-F_y(y)) \text{ for low risk}$$

5. Sum the contributions of the risk from other sources, if any.

A case is studied where two sites are located in a uniform source area, with $m_1=8.3, m_0=4, \beta=1.65, \sigma=0.5$ and subsequently 0.2 , resistance= 100cm/sec^2 and $\hat{\gamma}=7 \times 10^{-6}/\text{yr}/\text{km}^2$. The results for the events that at least one site fail and that two sites fail simultaneously are plotted in Fig. 23 and 24. In the figures the results obtained from using the

deterministic attenuation law are also plotted for comparison. As shown in Fig. 23 the consideration of the uncertainty in the attenuation increases the probability of at least one site failing for a given resistance and the level of the increase depends on the value of σ . At a certain spacing the probability of at least one site failing will be twice that probability for two coinciding sites. The spacing is very close to the spacing that will achieve a similar doubling of probability for the deterministic attenuation law case. In the case study $\epsilon = e^{3\sigma}$ is used to define the circular source area of influence. The potential earthquake source is modeled by a rectangle as was done in Sec.3.1. However, in using this rectangular area approximation, small segments of the source area which are excluded from the circular area are now included in the rectangular area. These sources, although contributing insignificantly to the risk, make the probability of two sites failing simultaneously nonzero even though the distance between the two sites is such that the two circular source areas are separated from each other, as shown in Fig.24. One can also see from this figure that for a given annual risk of two sites failing simultaneously, the probabilistic case needs a larger spacing between the two sites.

The conclusion from the above study is that the uncertainty term in the attenuation law should always be included in the risk study. The influence of considering this uncertainty term on the risk result depends on the magnitude of σ and the level of the site resistance relative to the upper bound and the lower bound of the earthquake magnitude.

3.3 Application

The objective of seismic risk analysis is to provide valuable information to decision makers so, provided with other information, they can make a good decision. This other information may include initial cost of a project, operating and maintenance cost, loss of operational function during repair of the system, impact on the community, human life loss and the quantification of relationships between the before mentioned factors and the spacing between sites. These are the main and difficult tasks in the decision making process.

The above study of seismic risk (Sec. 3.2) can be applied to a system of two facilities, such as power generating plants or water supply system, which will locate in a uniform source area, for an economic study of the system such as a benefit/

loss study and for decision making.

The following example is intended to give a crude description of a possible application of the risk results studied above. A two-power generating plant system is being planned for an earthquake prone region(uniform source area in this case). The resistances of these two plants are the same(e.g. 300 cm/sec²). From the seismic risk study one obtains the information regarding the annual risk of the event that one plant will fail and the annual risk of the event that two plants will fail simultaneously for each different spacing between these two plants. One would also need information about the loss due to each event, the initial cost, the operating cost, the relationship between the initial cost and the spacing ,and the relationship between the operating cost and the spacing. After obtaining all the information, the expected cost(ignoring discounting of future costs to present cost) during the expected life time T of the system can be expressed as:

$$\text{expected cost} = [C_1 p_1(d) + C_2 p_2(d) + C_3 f_1(d)] T + C_0 f_2(d) \quad (33)$$

where C_1 is the loss due to the event that only one facility fails*.

* C_1 and C_2 depend on the definition of failure

C_2 is the loss due to the event that two facilities fail simultaneously.*

C_3 is the annual operating-maintenance cost.

C_0 is the initial cost.

$p_1(d)$ is the annual seismic risk of only one facility fails and it can be obtained from the study in Sec.3.2

$p_2(d)$ is the annual seismic risk of two facilities fail simultaneously.

$f_1(d)$ is the relationship which expresses the increase of operating cost with respect to the distance between two facilities.

$f_2(d)$ is the relationship which expresses the increase of initial cost with respect to distance between two facilities.

In this example C_1 and C_2 are assumed as the total loss (repair cost, community loss due to the facilities failure). The relative weights for $C_0, C_1, C_2,$ and C_3 are 2, 200, 1000 and 0.001, respectively. In an actual study these values would have to be obtained from a hazard study. The same linear relationship was used here for $f_1(d)$ and $f_2(d)$ because of its simplicity, but it may be unrealistic for an actual study. The quantification of the relationship between the initial cost and/or operating cost and the spacing has also to be established by a **thorough**

study. The seismic risk results for these two facilities are based on the following information: upper bound of the epicentral magnitude $m_1=8.3$, lower bound $m_0=4$, resistances of the two facilities $R=300\text{cm/sec}^2$, the standard deviation of the uncertainty term in the attenuation law $\sigma=0.2$ and Donovan's⁽¹⁰⁾ attenuation law. The results are plotted in Figure 25. One can see that the optimal spacing in this example is 30 km. At this spacing, the total expected cost will be at a minimum.

3.4 Conclusion

In Sec. 3.1 it was found that the seismic risk study for a spatially distributed system is very sensitive to the attenuation law constants b_2 and b_3 , but is less sensitive to b_1 . The consideration of the uncertainty in the attenuation law increases the seismic risk obtained by using the deterministic attenuation law. The level of the increase depends on the magnitude of the standard deviation σ of the normally distributed variate $\ln \epsilon$ and the level of the resistance relative to the upper bound and lower bound of the epicentral magnitude. When σ is small the seismic risk obtained by using the probabilistic attenuation law is essentially the

same as that obtained by using the deterministic attenuation law. The computer program used in the study has the capability of dealing with more general cases, such as a system of more than two spatially distributed sites with different resistance for each site. Thus the application of the study in Sec.3.3 can be more versatile. The cost estimates and the quantification of certain relationships such as the relationship of the initial cost and the spacing between sites have to be studied more thoroughly in order to obtain more realistic and accurate results for the purpose of decision analysis.

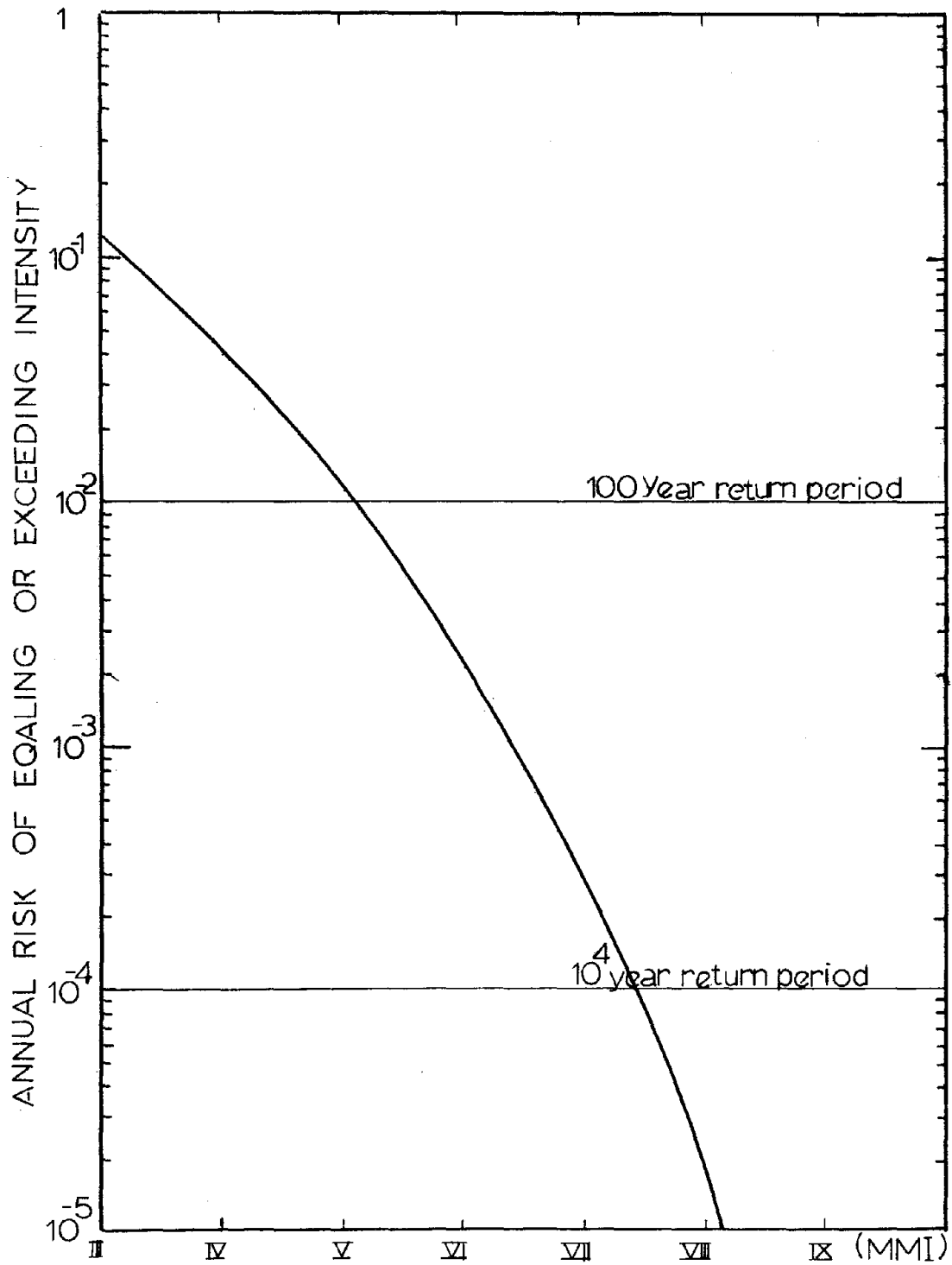


FIG.1:SEISMIC RISK CURVE

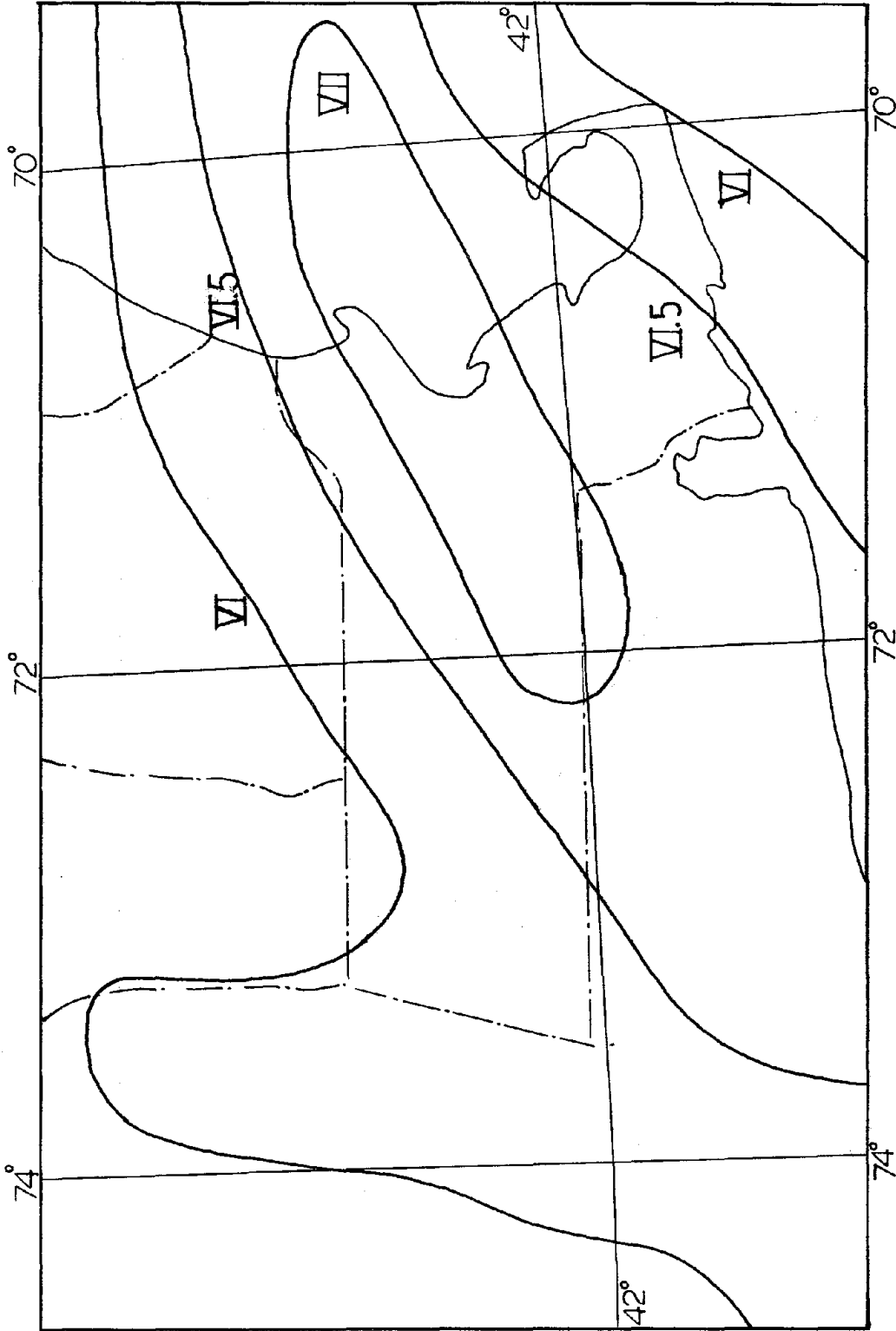


FIG.2 SEISMIC RISK MAP FOR 1000 YR. RETURN PERIOD

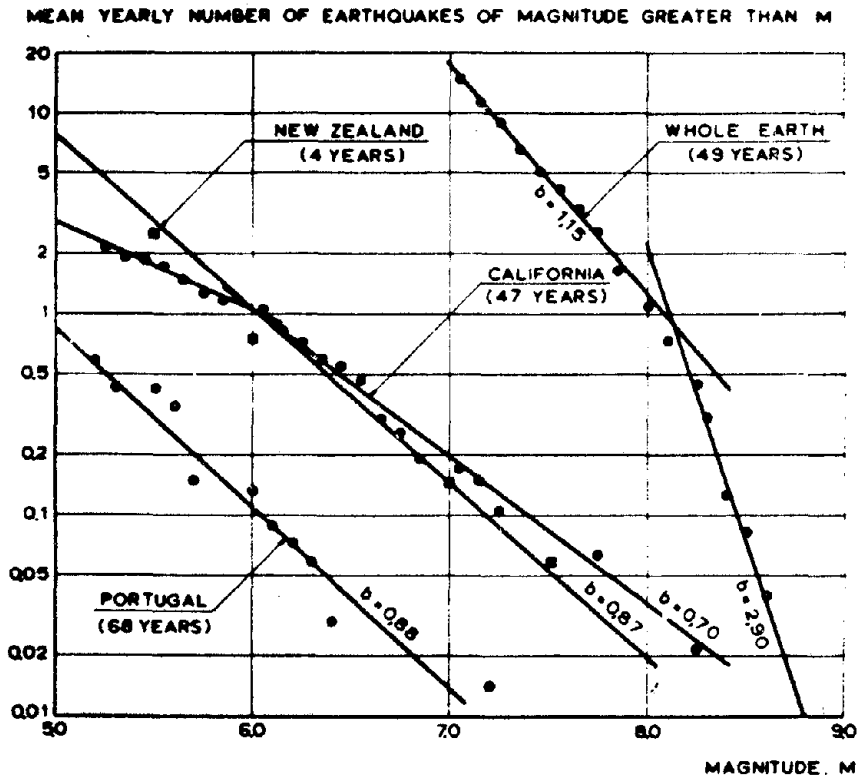


FIG. 3 MEAN YEARLY NUMBER OF EARTHQUAKES OF MAGNITUDES GREATER THAN M FOR DIFFERENT REGIONS⁽²⁾

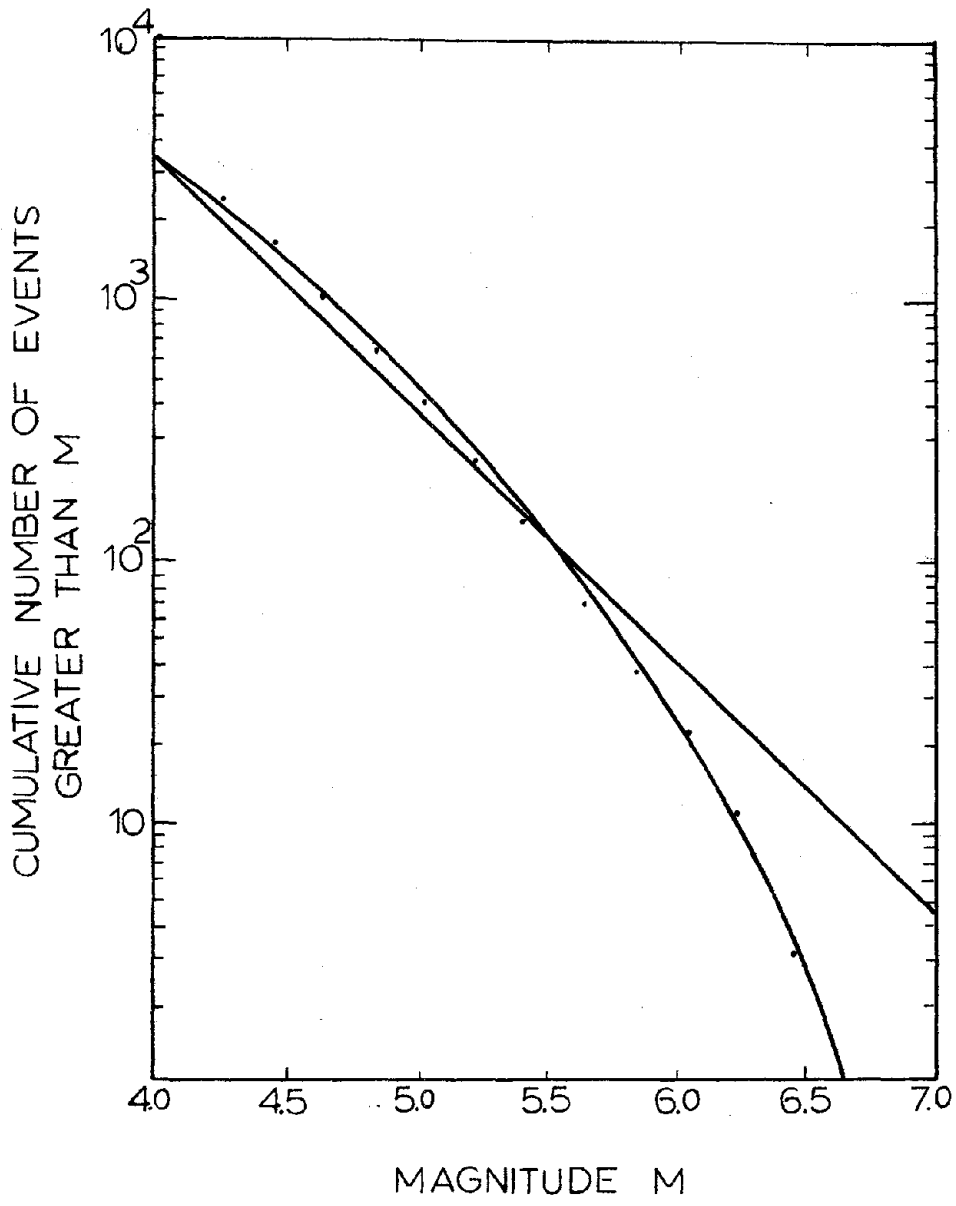


FIG. 4 FREQUENCY MAGNITUDE
RELATIONSHIP

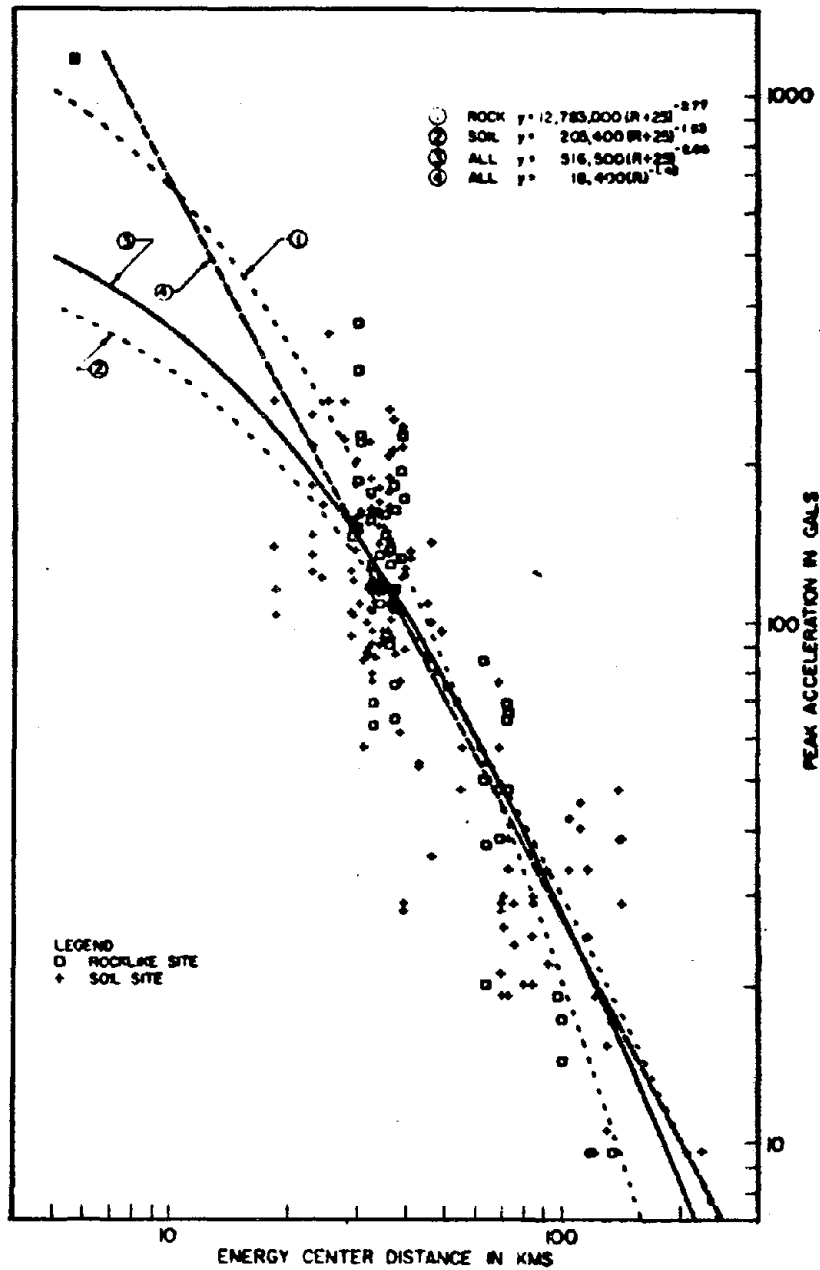


FIG.5 LEAST SQUARES TO PEAK
 GROUND ACCELERATIONS
 FEB.9,1971 SAN FERNANDO
 EARTHQUAKE

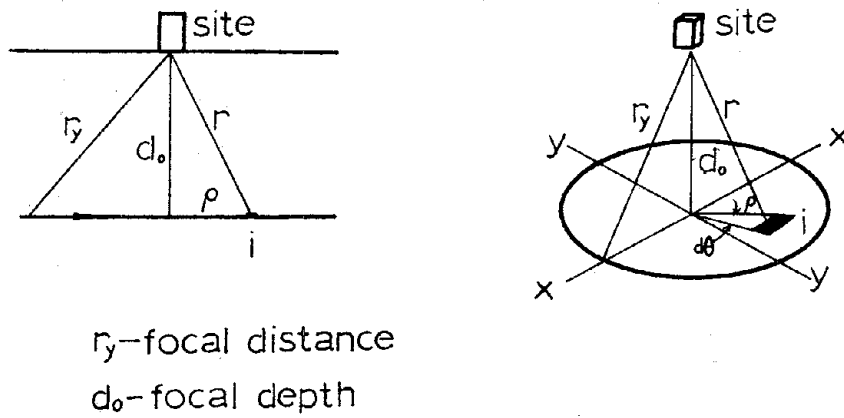


FIG. 6 SOURCE-SITE GEOMETRY

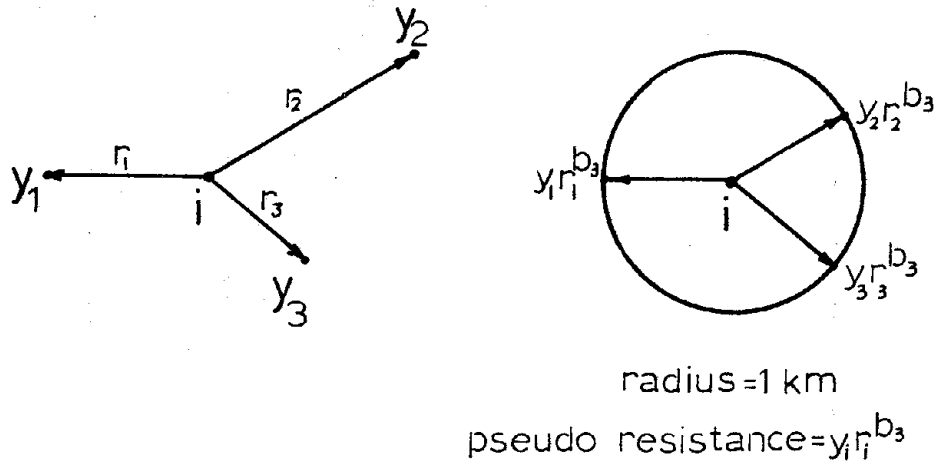


FIG. 7 SPATIALLY DISTRIBUTED SYSTEM⁽²⁵⁾

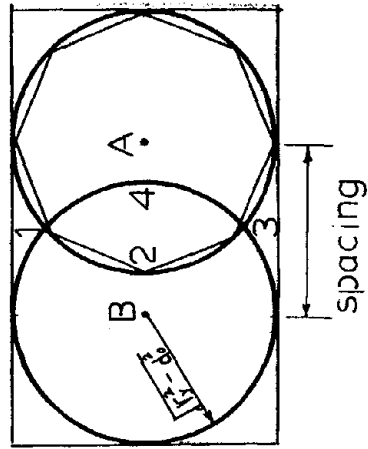


FIG. 8 MODELING OF UNIFORM SOURCE AREA

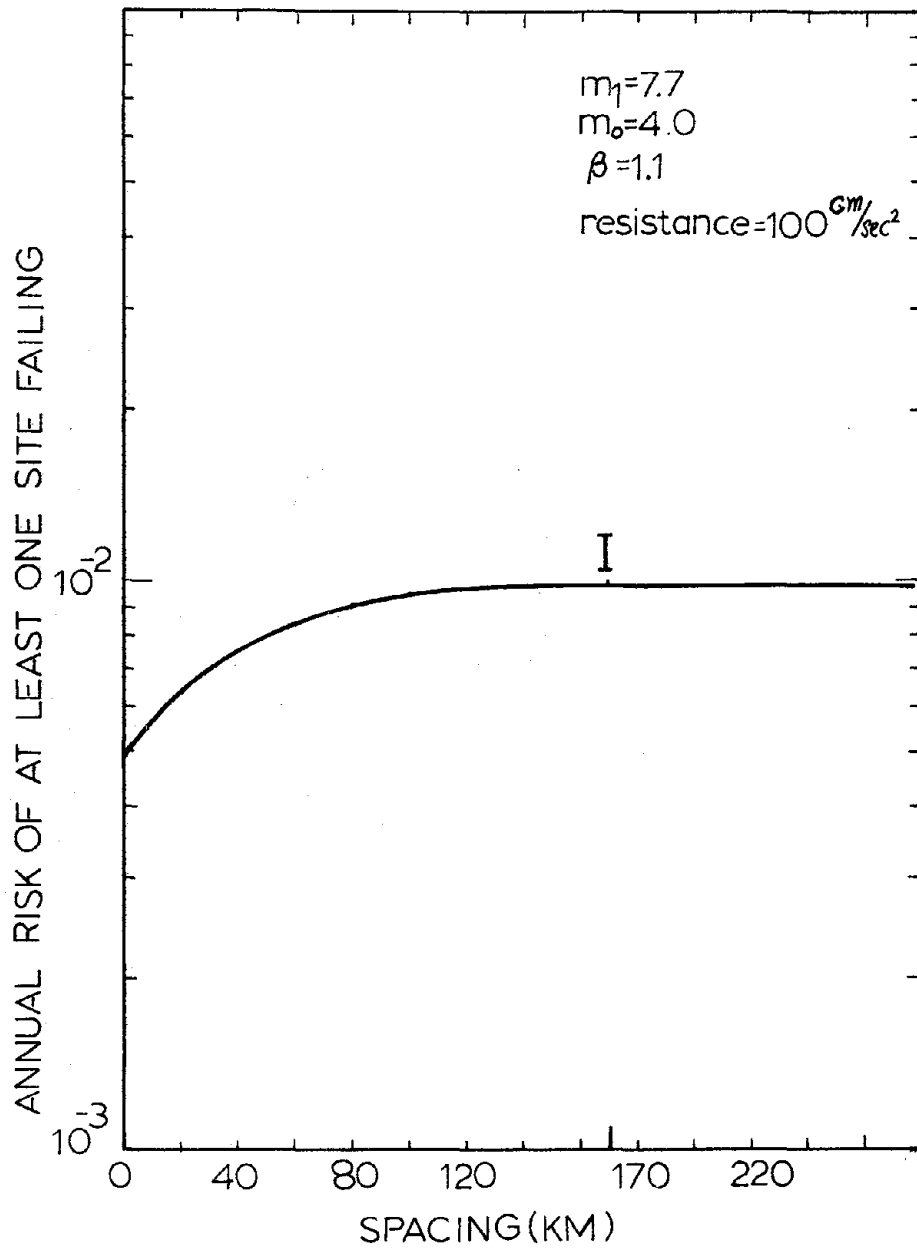


FIG. 9 RISK CURVE OF TWO-SITE CASE

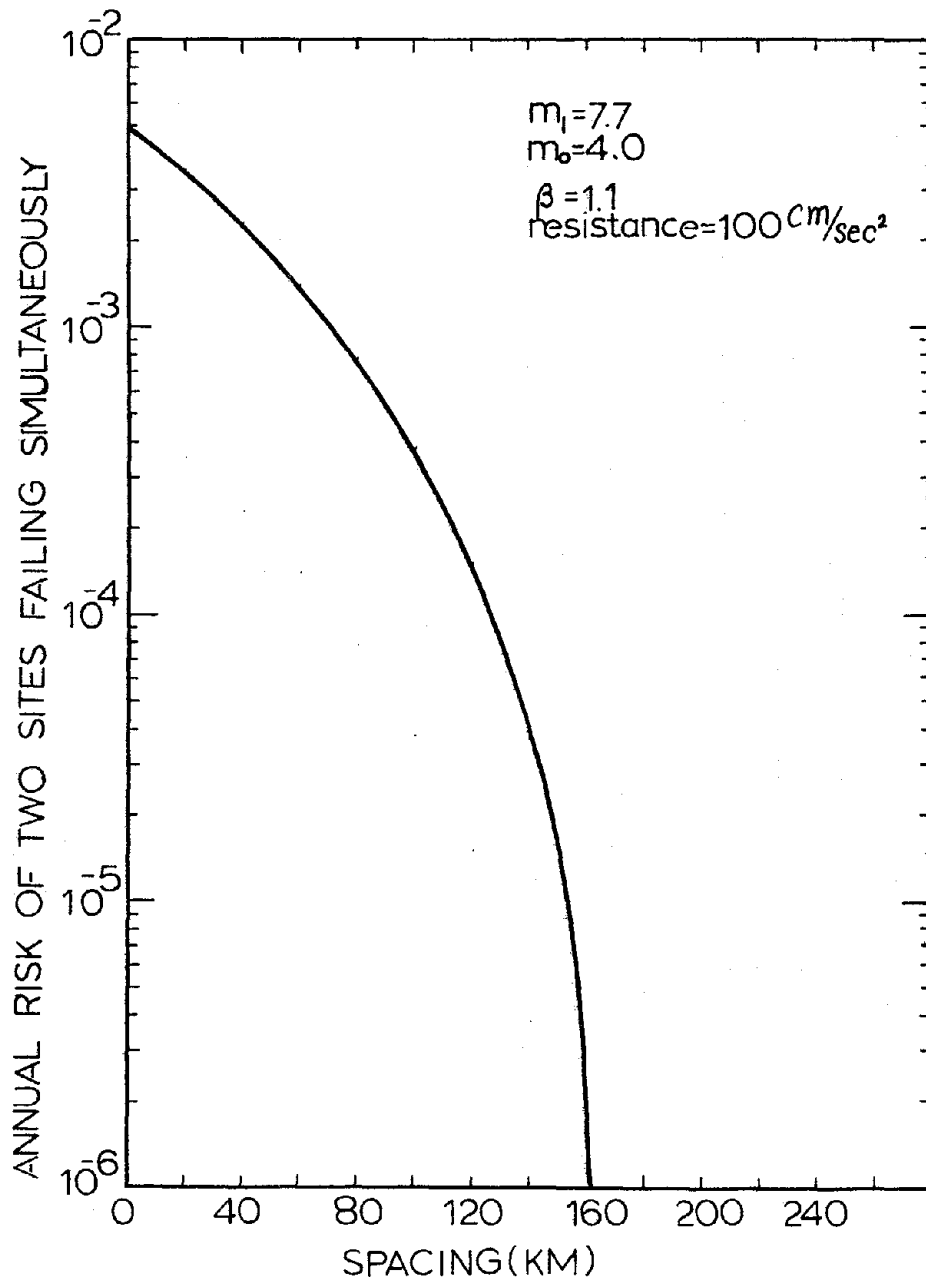


FIG.10 RISK CURVE OF TWO-SITE CASE

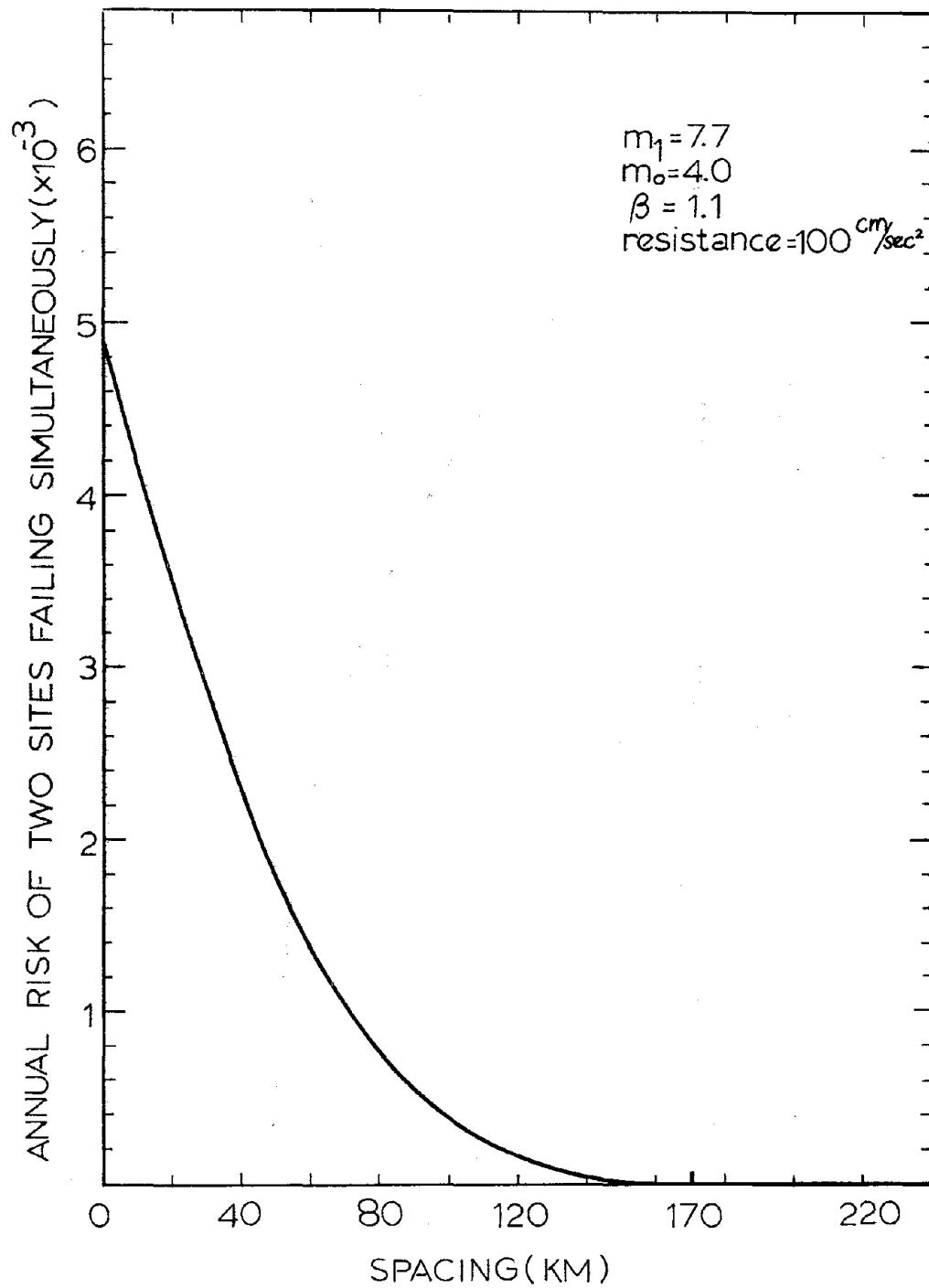
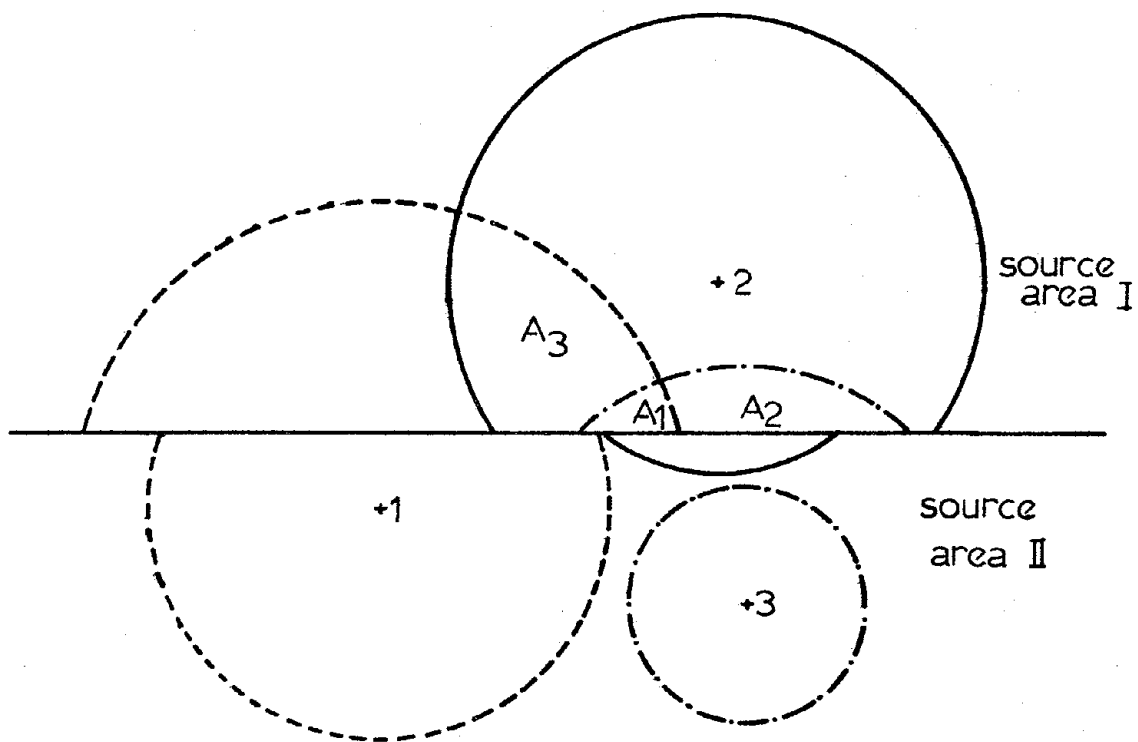
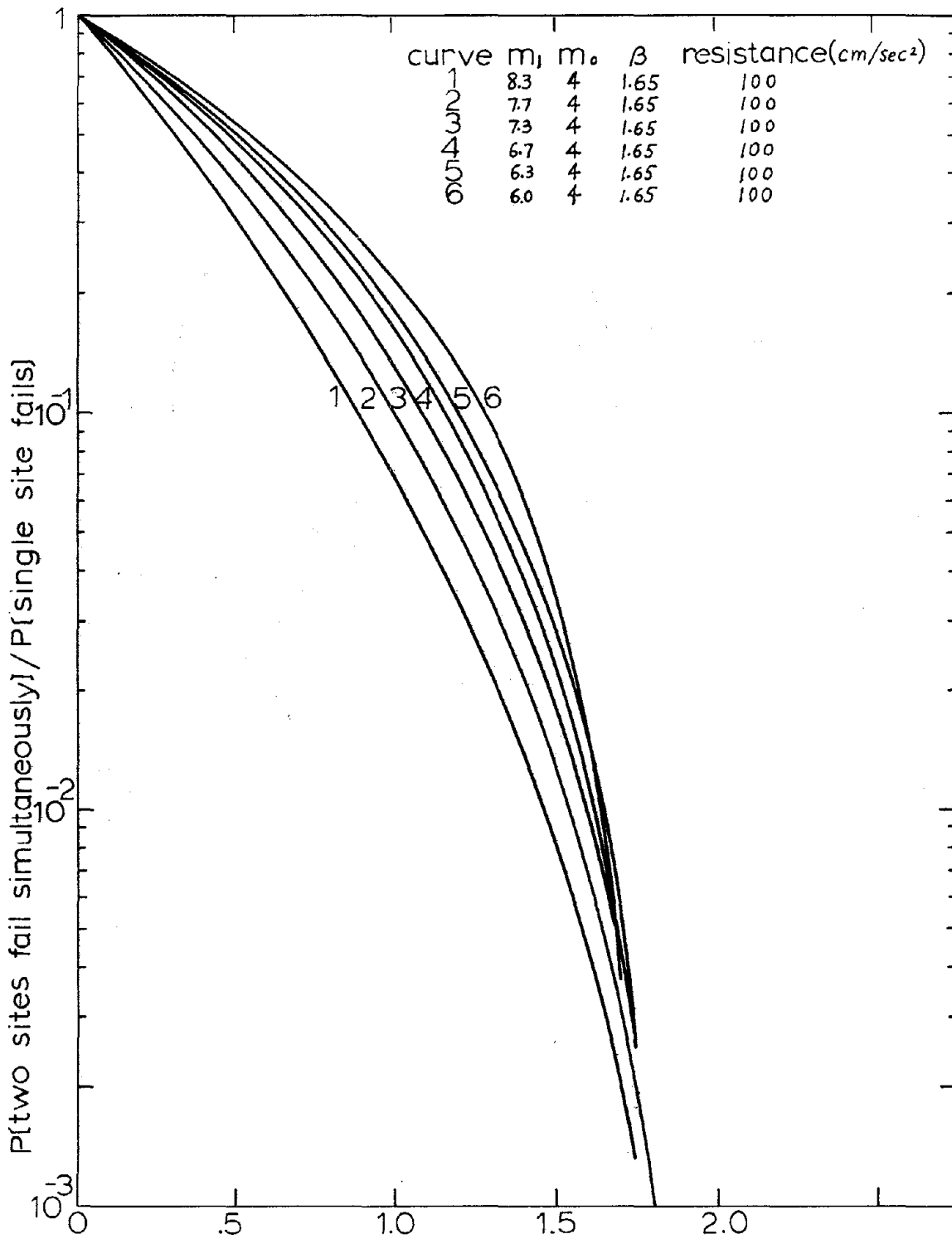


FIG. 11 RISK CURVE OF TWO-SITE CASE



resistance 1 < resistance 2 < resistance 3

FIG.12 GENERAL SOURCE-SITE GEOMETRY



spacing/radius of circular source area ($\sqrt{r_y^2 - d^2}$)

FIG.13 NORMALIZED RISK CURVE

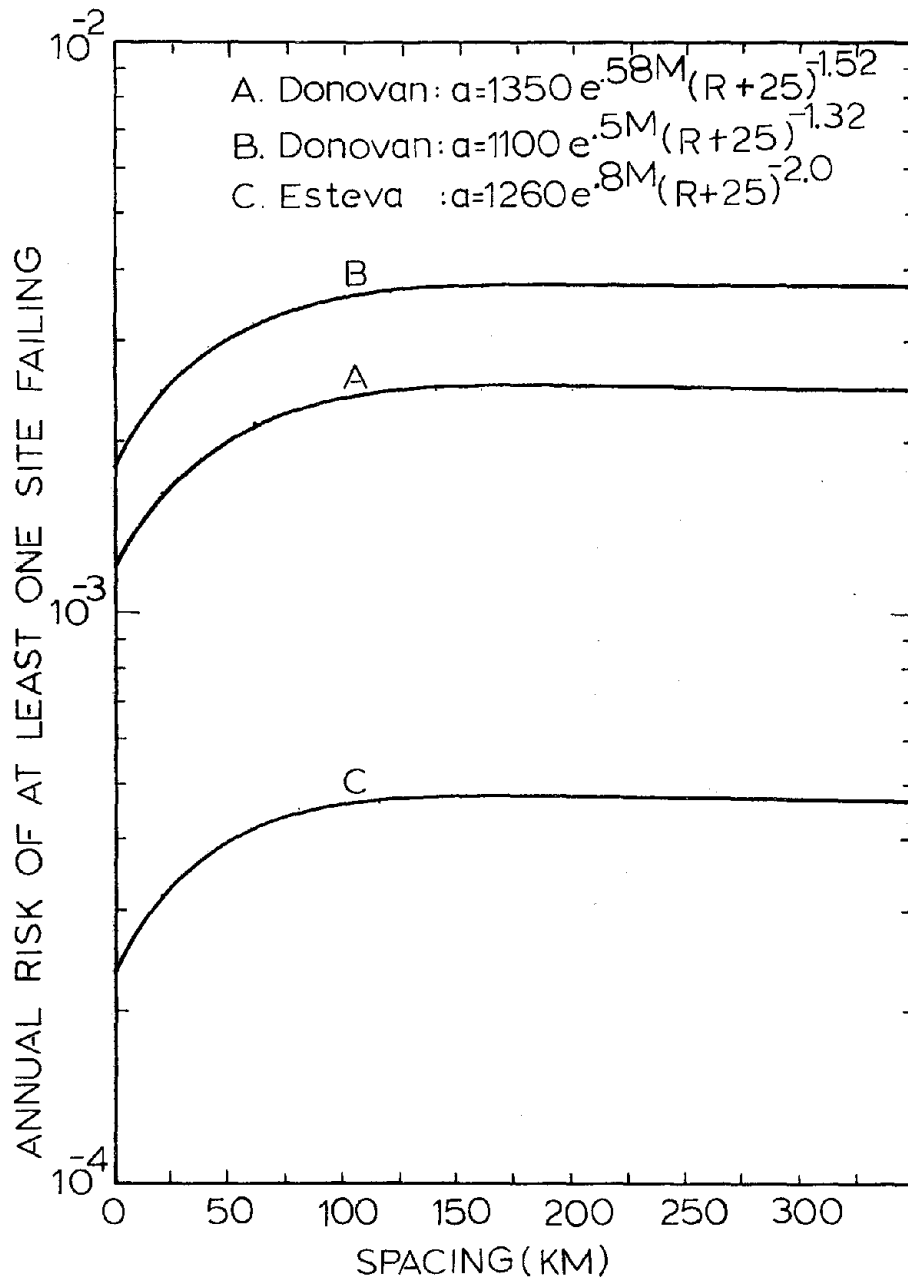


FIG.14 SENSITIVITY STUDY

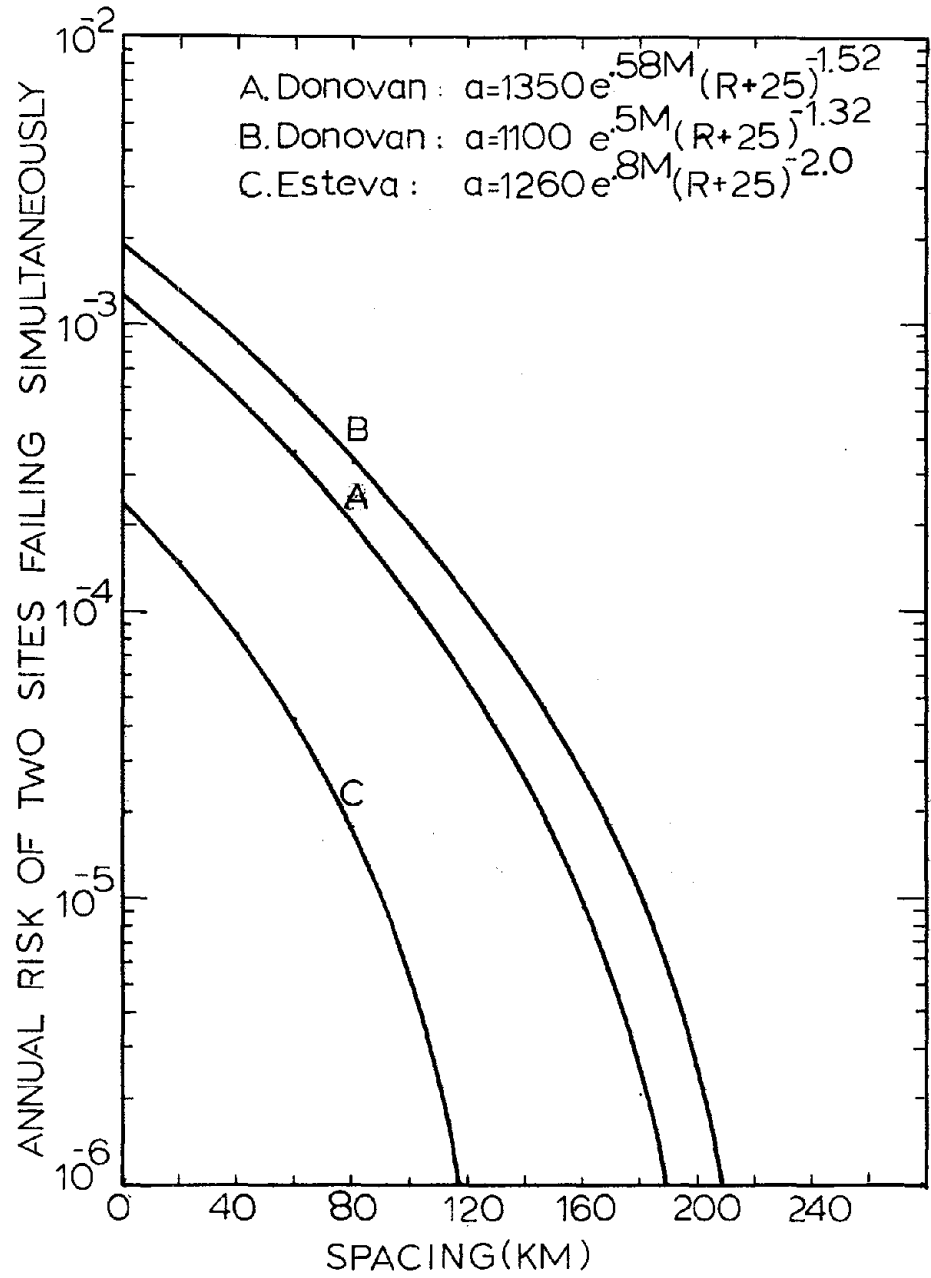


FIG.15 SENSITIVITY STUDY

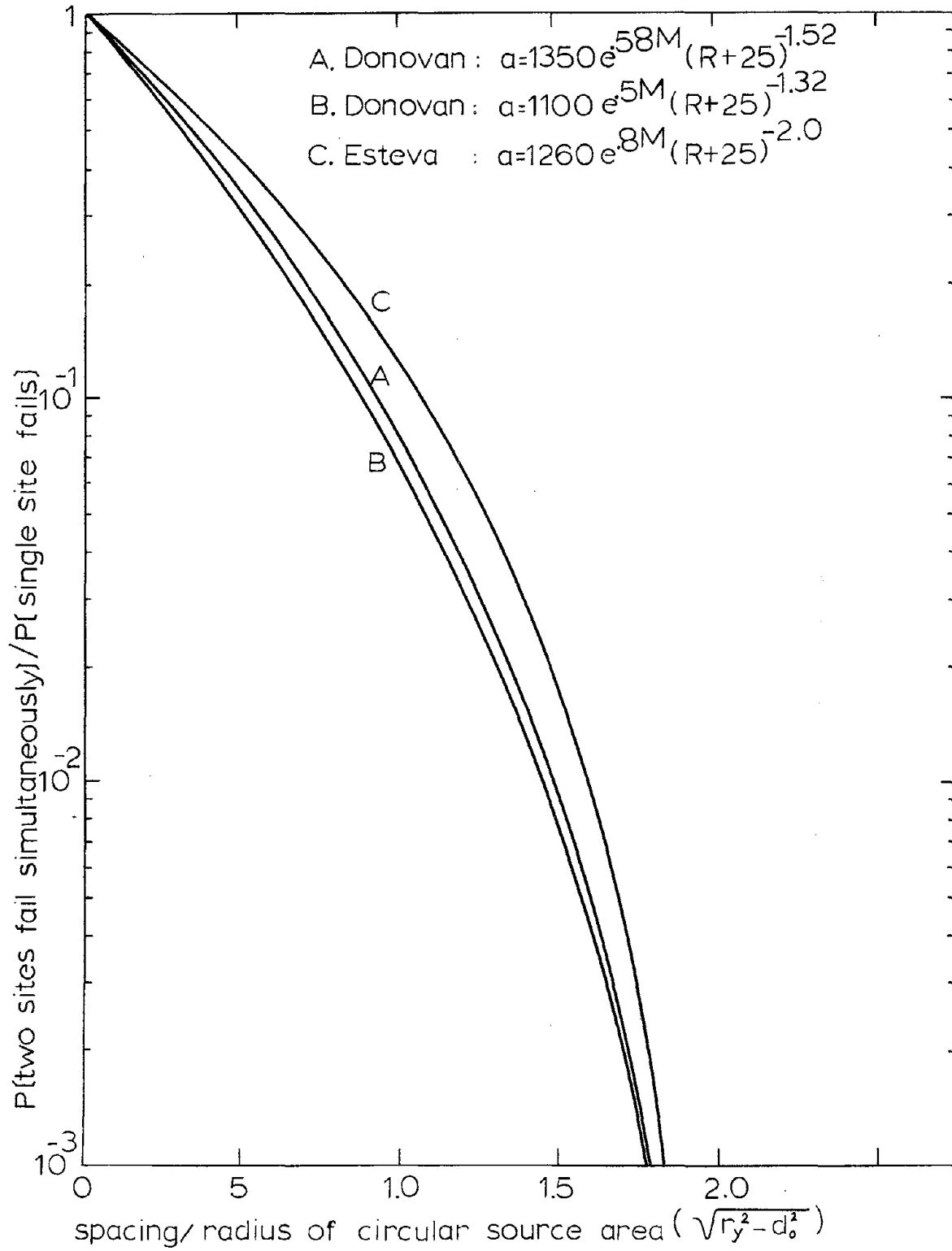


FIG.16 NORMALIZED RISK CURVE

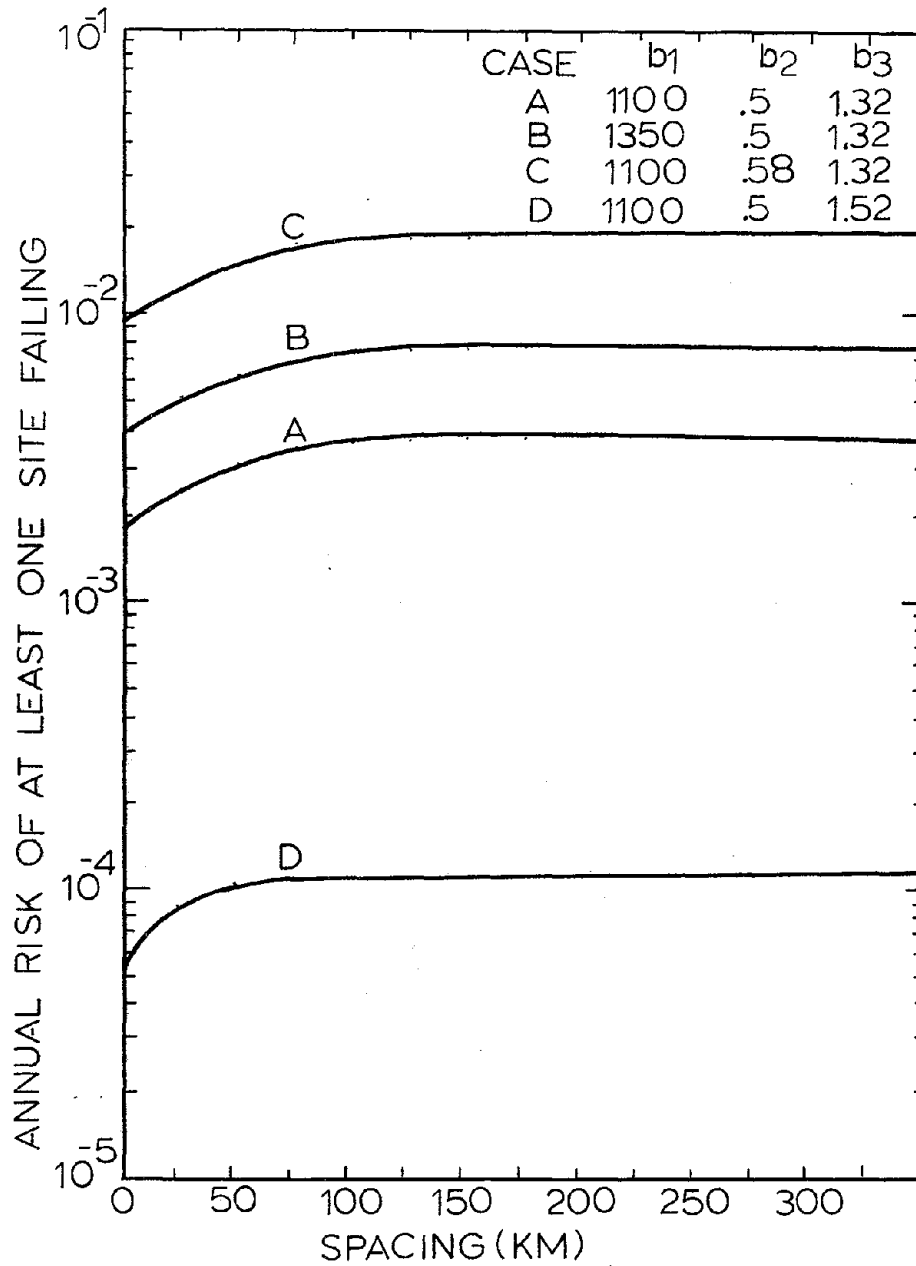


FIG.17 SENSITIVITY STUDY

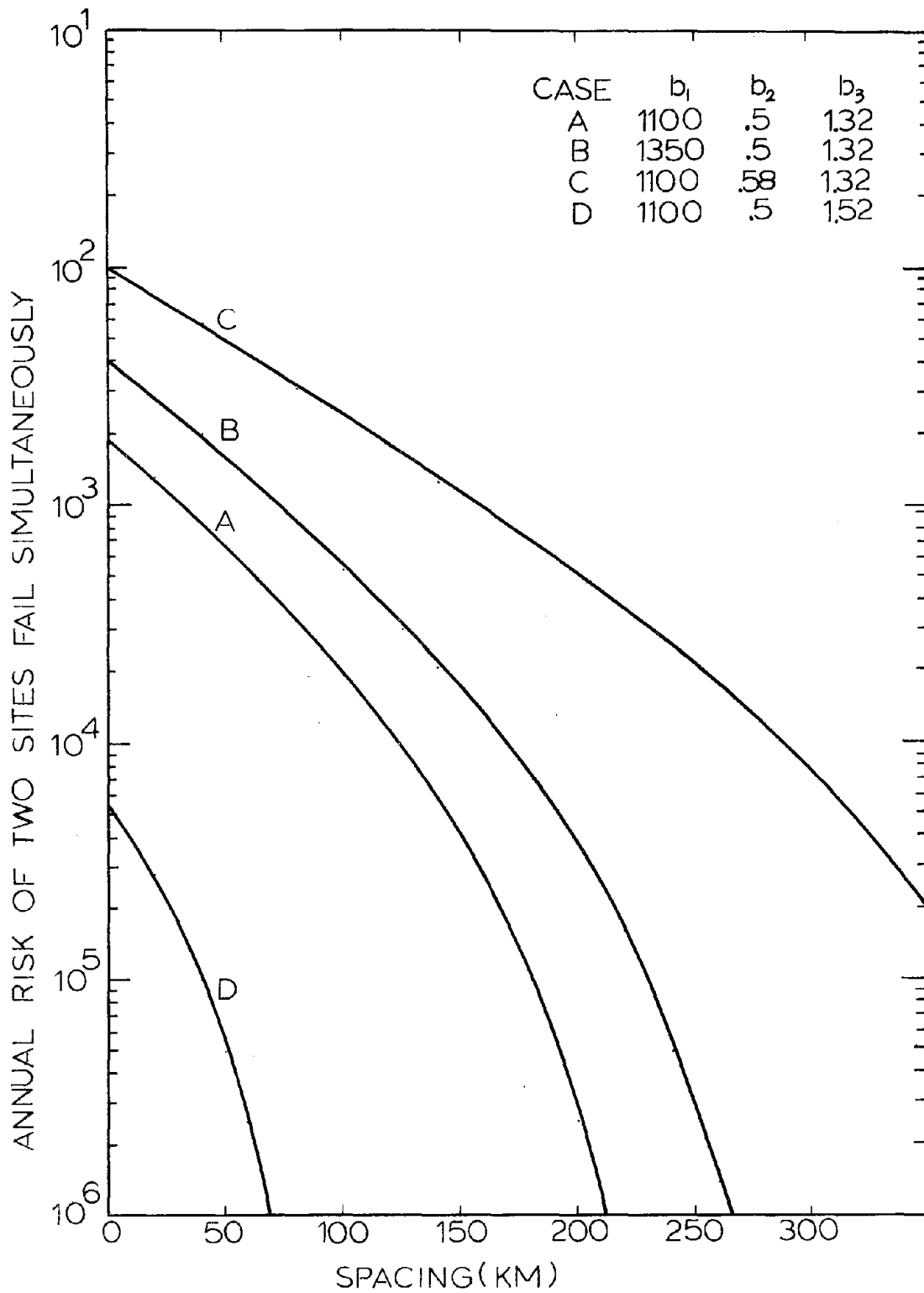


FIG.18 SENSITIVITY STUDY

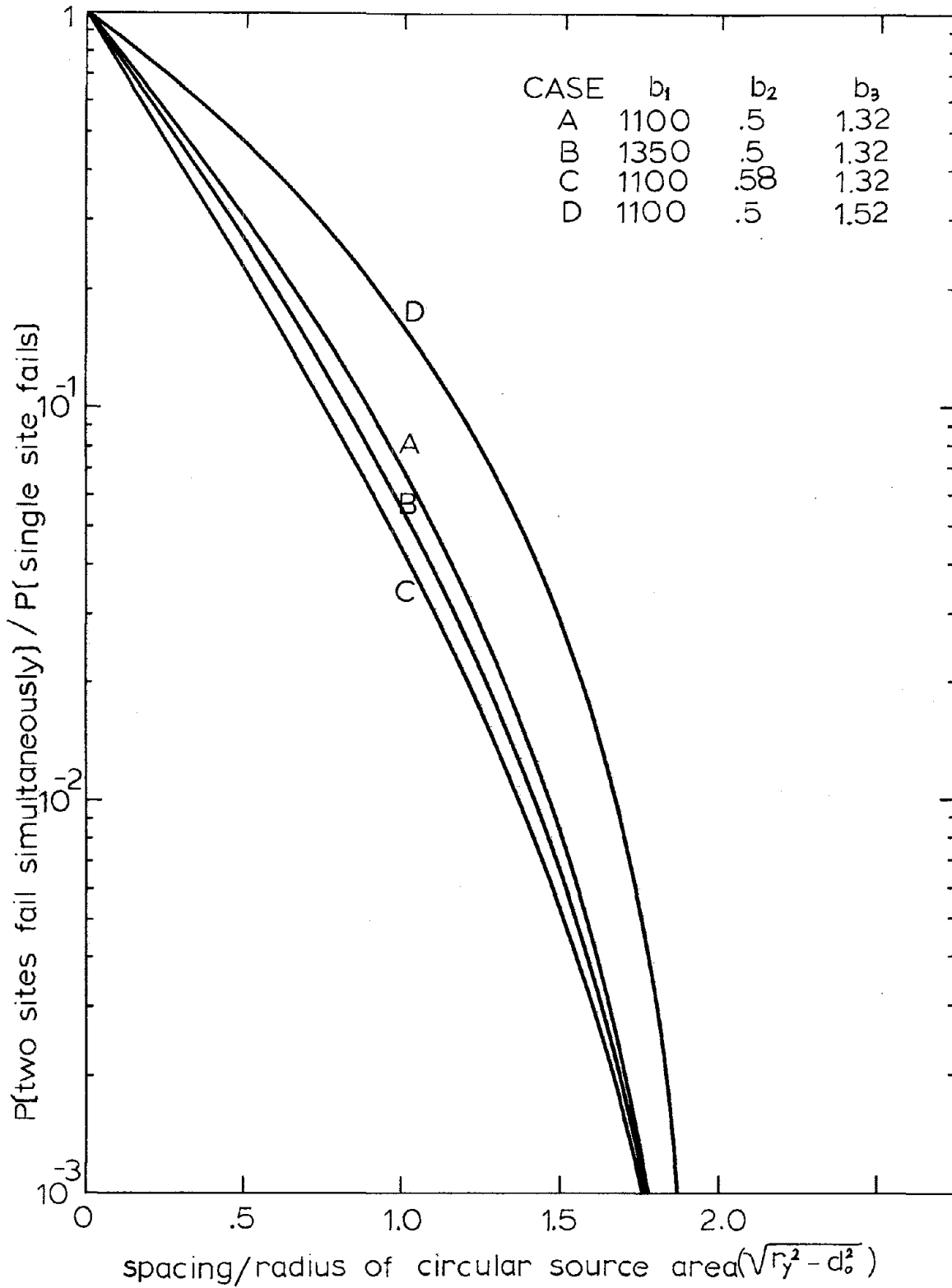


FIG.19 NORMALIZED RISK CURVE

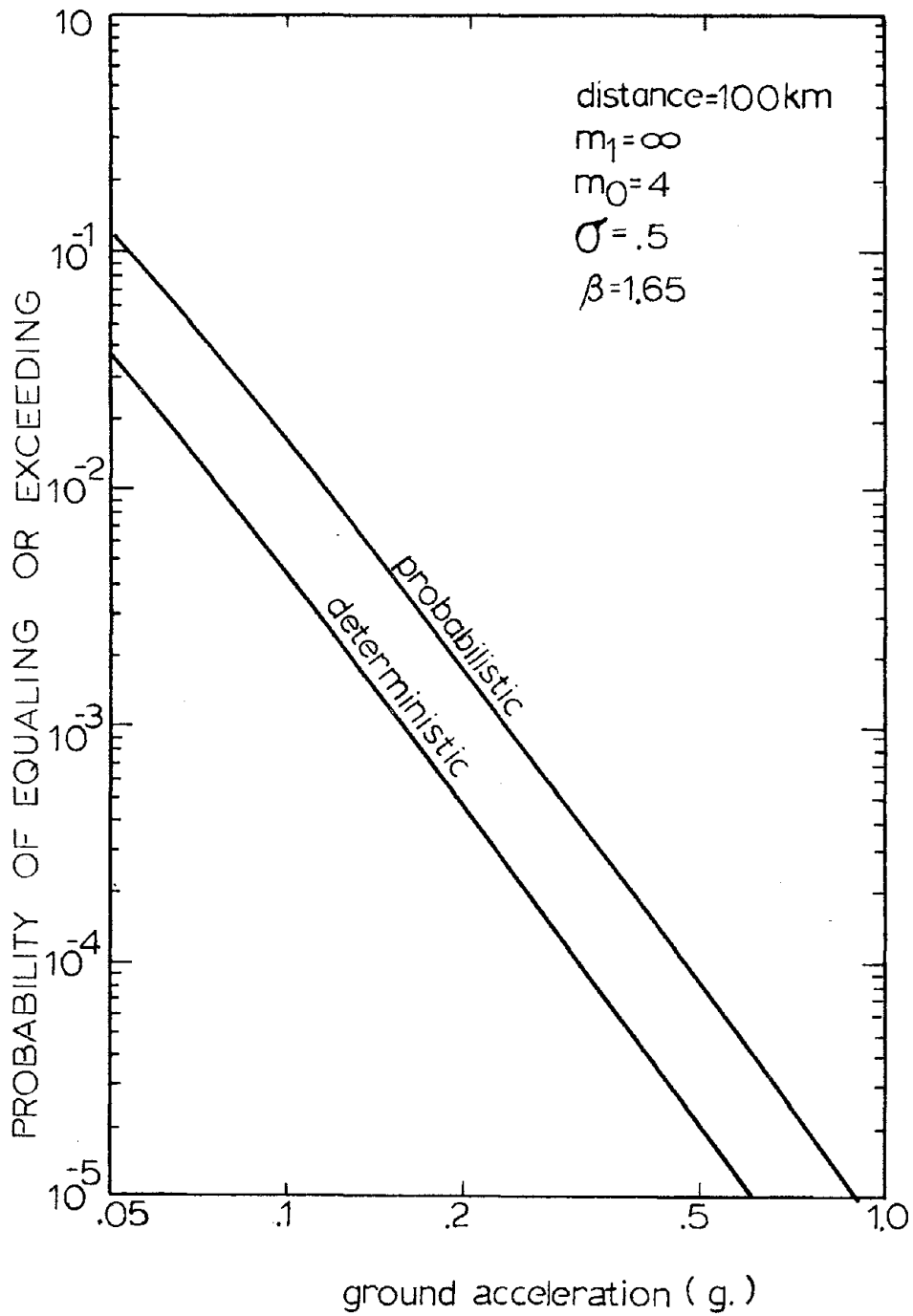


FIG. 20 RISK CURVE

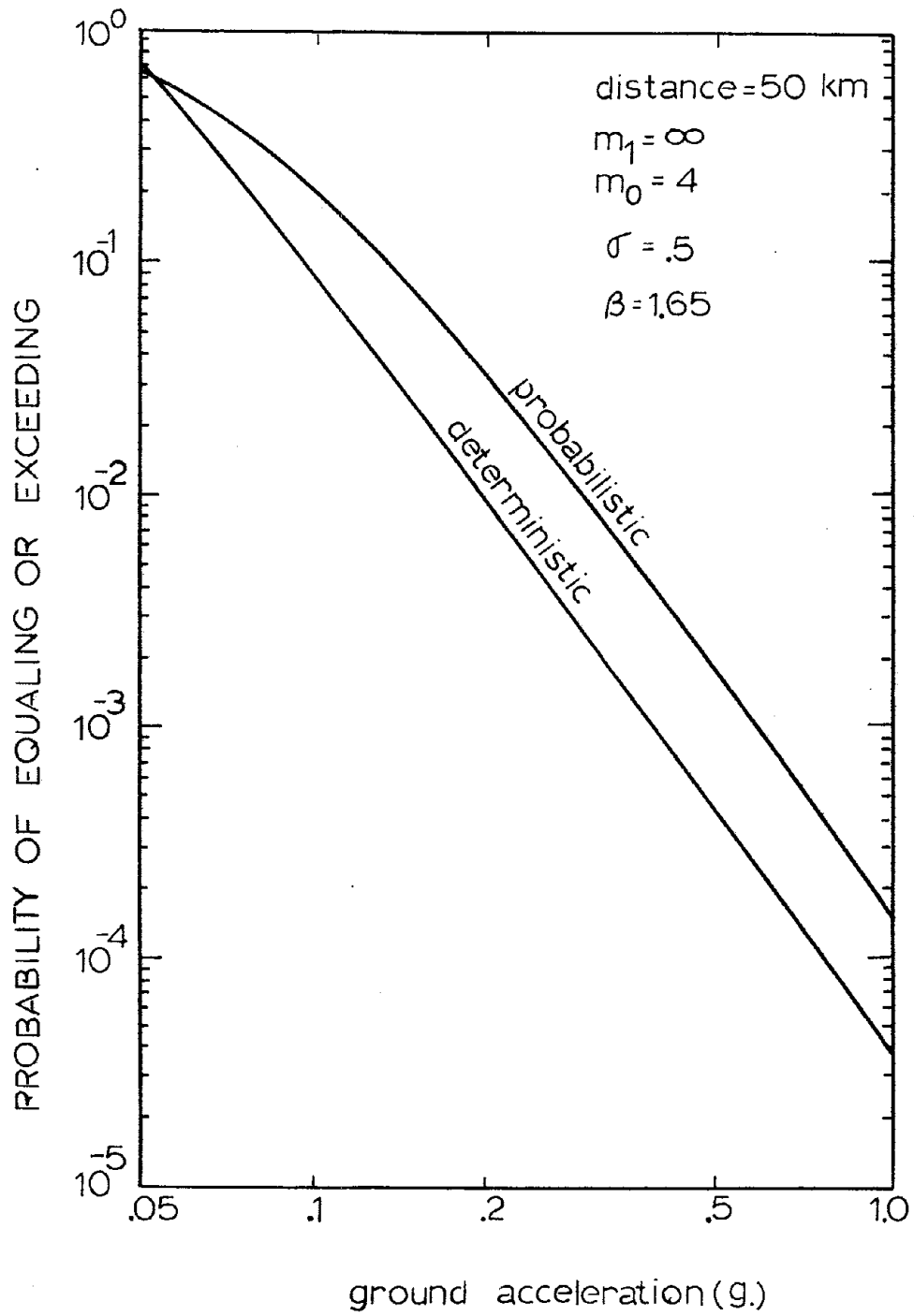


FIG.21 RISK CURVE

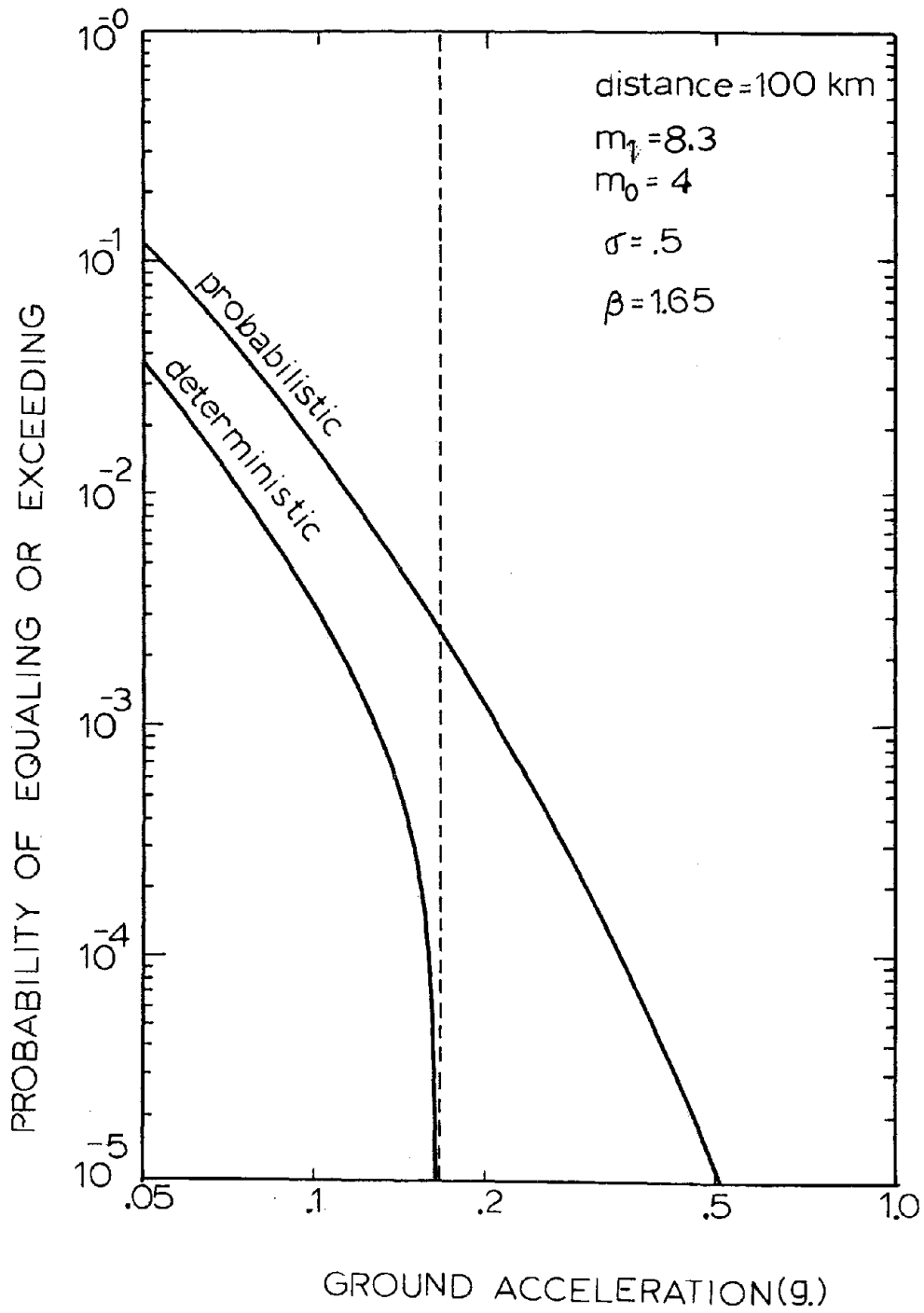


FIG.22 RISK CURVE

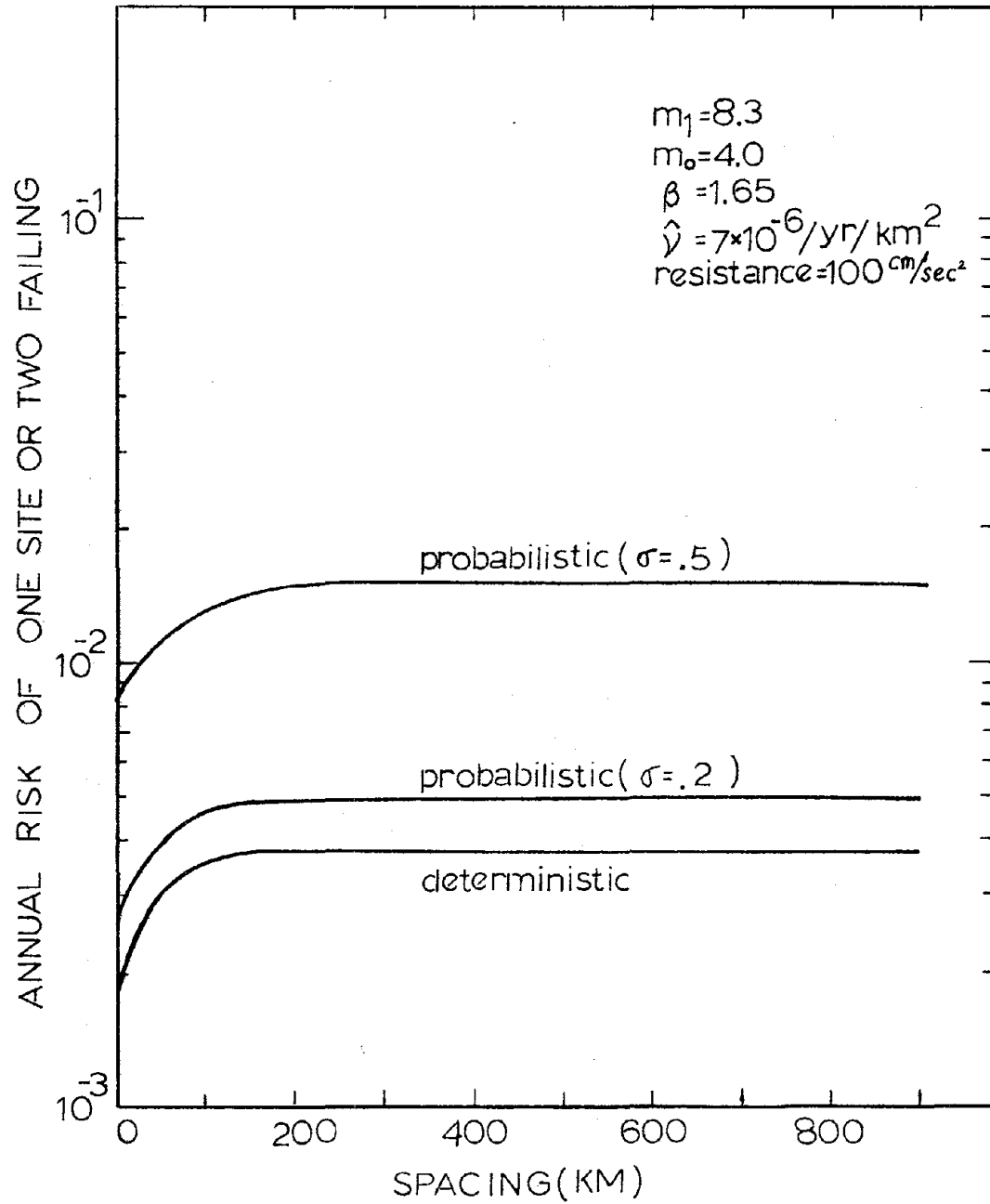


FIG.23 SEISMIC RISK CURVE OF TWO-SITE CASE

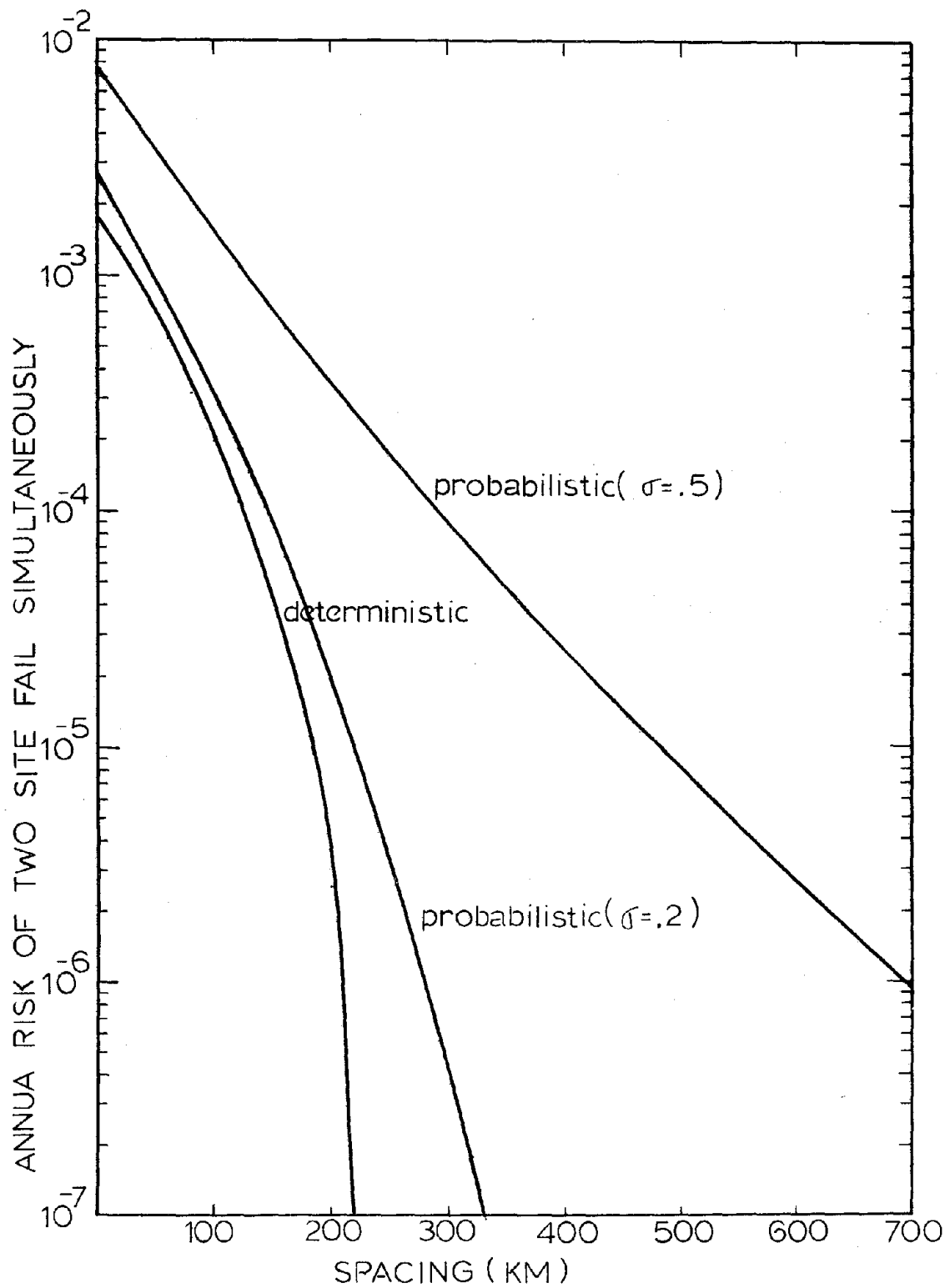


FIG.24 SEISMIC RISK CURVE OF TWO-SITE CASE

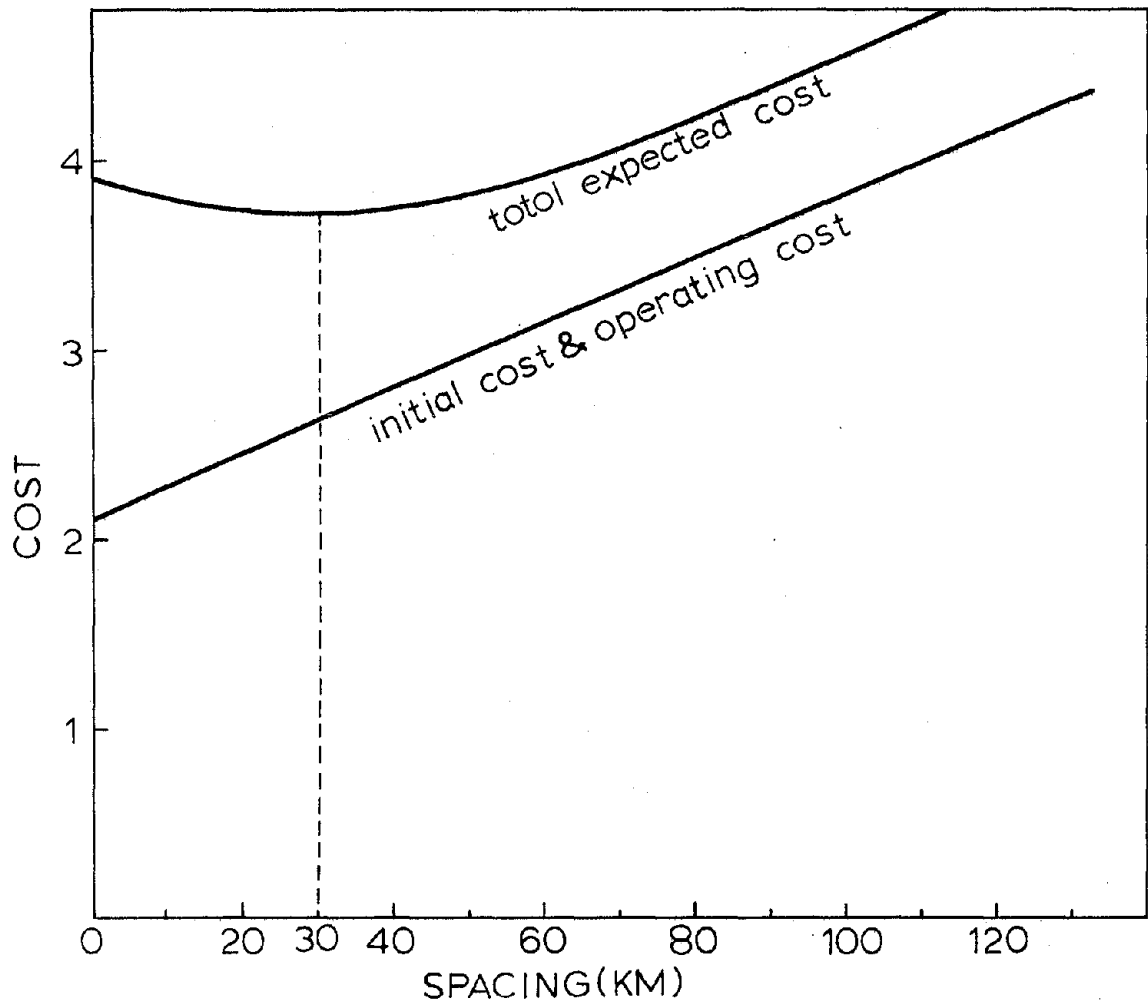


FIG.25 COST BENEFIT ANALYSIS

ϵ	radius(km)	P[at least one fail]	P[both sites fail]
e^0	27	1.85×10^{-4}	6.97×10^{-4}
e^1	61	2.78×10^{-4}	1.15×10^{-5}
e^2	104	2.95×10^{-4}	1.30×10^{-5}
e^3	166	2.97×10^{-4}	1.32×10^{-5}
e^4	256	2.97×10^{-4}	1.32×10^{-5}
$\sigma = 0.5$ spacing = 100 Km $m_1 = 8.3$ $m_0 = 4$ $R = 300 \text{ cm/sec}^2$			

TABLE 2 STABILITY STUDY

ϵ	radius(km)	P[at least one fail]	P[both sites fail]
e^0	215	5.27×10^{-2}	3.70×10^{-2}
e^1	326	5.32×10^{-2}	3.74×10^{-2}
e^2	489	5.32×10^{-2}	3.74×10^{-2}
e^3	729	5.32×10^{-2}	3.74×10^{-2}
e^4	1072	5.32×10^{-2}	3.74×10^{-2}
$\sigma = 0.5$ spacing = 20 Km $m_1 = 8.3$ $m_0 = 4$ $R = 50 \text{ cm/sec}^2$			

TABLE 3 STABILITY STUDY

ϵ	radius(km)	P[at least one fail]	P[both sites fail]
e^0	115	8.82×10^{-3}	5.35×10^{-3}
e^1	182	9.17×10^{-3}	5.59×10^{-3}
e^2	278	9.24×10^{-3}	5.64×10^{-3}
e^3	419	9.24×10^{-3}	5.65×10^{-3}
e^4	624	9.24×10^{-3}	5.65×10^{-3}
$\sigma = 0.5$ spacing = 20 Km $m_1 = 8.3$ $m_0 = 4$ $R = 100 \text{ cm/sec}^2$			

TABLE 4 STABILITY STUDY

ϵ	radius(km)	P[at least one fail]	P[both sites fail]
e^0	115	1.41×10^{-2}	1.85×10^{-4}
e^1	182	1.45×10^{-2}	2.13×10^{-4}
e^2	278	1.46×10^{-2}	2.22×10^{-4}
e^3	419	1.46×10^{-2}	2.23×10^{-4}
e^4	624	1.46×10^{-2}	2.23×10^{-4}
$\sigma = 0.5$ spacing = 230 Km $m_1 = 8.3$ $m_0 = 4$ $R = 100 \text{ cm/sec}^2$			

TABLE 5 STABILITY STUDY

ϵ	radius(km)	P[at least one fail]	P[both sites fail]
e^0	115	3.60×10^{-3}	1.97×10^{-4}
e^1	117	3.60×10^{-3}	1.97×10^{-4}
e^2	119	3.60×10^{-3}	1.97×10^{-4}
e^3	122	3.60×10^{-3}	1.97×10^{-4}
e^4	124	3.60×10^{-3}	1.97×10^{-4}
$\sigma = 0.02$ spacing = 100 Km $m_1 = 8.3$ $m_0 = 4$ $R = 100 \text{ cm/sec}^2$			

TABLE 6 STABILITY STUDY

ϵ	radius(km)	P[at least one fail]	P[both sites fail]
e^0	115	2.50×10^{-2}	4.45×10^{-3}
e^1	216	2.73×10^{-2}	5.21×10^{-3}
e^2	386	2.78×10^{-2}	5.42×10^{-3}
e^3	675	2.79×10^{-2}	5.42×10^{-3}
e^4	1165	2.79×10^{-2}	5.42×10^{-3}
$\sigma = 0.7$ spacing = 100 Km $m_1 = 8.3$ $m_0 = 4$ $R = 100 \text{ cm/sec}^2$			

TABLE 7 STABILITY STUDY

References

1. Algermissen, S.T. and D.M. Perkins (1972) "A Technique for Seismic Zoning: General Consideration and Parameters" Proc. Inter. Conf. Microzonation for Safer Construction, Seattle, Washington 1972.
2. Berges, J. Ferry and M. Castanheta (1971) Structural Safety, Chapter 17.
3. Cornell, C.A. (1964) "Stochastic Process Models in Structural Engineering," Dept. of Civil Engineering Technical Report No. 34, Stanford University.
4. Cornell, C.A. (1968) "Engineering Seismic Risk Analysis," Bulletin of Seismological Society of America, Vol.58, No. 5.
5. Cornell, C.A. and Erik H. Vanmarcke (1969) "The Major Influences on Seismic Risk" Proc. of Fourth World Conf. on Earthquake Engineering.
6. Cornell, C.A. and Erik H. Vanmarcke (1969) "Analysis of Uncertainty in Ground Motion and Structural Response Due to Earthquakes" M.I.T. Civil Engineering Report R.69-24.
7. Cornell, C.A. (1970) "Probabilistic Analysis of Damage to Structures Under Seismic Loads," Dynamic Waves in Civil Engineering, edited by D.A. Howells, Wiley-Interscience (1971)
8. Cornell, C.A. and H.A. Merz (1974) "A Seismic Risk Analysis of Boston" M.I.T. Civil Engineering Report R74-2.
9. Cornell, C.A. (1974) "A Note on General Procedures for Seismic Risk Analysis of Spatially Distributed Systems" M.I.T. Civil Engineering Report, Internal Study Report No. 47.
10. Donovan, Neville C. (1974) "A Statistical Evaluation of Strong Motion Data Including the February 9, 1971 San Fernando Earthquake." Fifth World Conf. on Earthquake Engineering, Rome

11. Esteva, L. and E. Rosenblueth (1964) "Spectra of Earthquakes at Moderate and Large Distance" Society Mexico de Ing. Sismica, Vol II, No. 1 pp. 1-18, Mexico.
12. Esteva, L. (1969) "Seismicity Prediction, A Bayesian Approach" Proc. of Fourth World Conf. on Earthquake Engineering, Chile.
13. Esteva, L. (1970) "Seismic Risk and Seismic Design Decision" Seismic Design for Nuclear Power Plants, Hansen edited. M.I.T. Press.
14. Kallberg, K.T. (1969) "Seismic Risk in Southern California" M.I.T. Civil Engineering Report R69-31.
15. Kantorovich, L.V., Keilis-Borok, V.I. and Molchan, G.M. (1974) "Seismic Risk and Principles of Seismic Zoning" M.I.T. Civil Engineering Internal Study Report No. 43 translated from Russian.
16. Keilis-Borok, V.I., T.L. Konrod and G.M. Molchan (1974) "Algorithm for the Estimation of Seismic Risk" M.I.T. Internal Study Report, No. 46, translated from Russian.
17. Lomnitz, Cinna (1969) "An Earthquake Risk Map of Chile," Fourth World Conf. on Earthquake Engineering, Chile.
18. Milne, W.G. (1971) "Earthquake Zoning in Canada" Canadian National Engineering Conference, Vancouver, Canada.
19. Merz, H.A. and Cornell, C.A. (1973) "Seismic Risk Analysis Based on a Quadratic Magnitude-Frequency Law." Bulletin of the Seismological Society of America, Vol.63 No. 6, pp. 1999-2006, Dec. 1973.
20. Oliveira, Carlos S. (1974) "Seismic Risk Analysis" Report No. EERC 74-1 University of California, Berkeley.
21. Panoussis, George (1974) "Seismic Reliability of Lifeline Networks," M.I.T. Civil Engineering Dept. Report No. 15.
22. Richter, C.F. and Gutenberg, B. (1942) "Earthquake Magnitude, Intensity, Energy and Acceleration" Bulletin of the Seismological Society of America, Vol 32, pp. 163-191.

23. Shah, H.C. and Vagliente, V.N. (1972) "Forecasting the Risk Inherent in Earthquake Resistant Design" Proc. International Conf. on Microzonation, Vol. 2.
24. Schumacker, Betsy (1975) "Nuclear Power Plants and the Operating Basis Earthquake - Phase I" M.I.T. Internal Study Report No. 51.
25. Taleb-Agha, Ghiath and Klaus Hein (1975) "Multiple Failure Risk of Spatially Distributed Structures" M.I.T. Internal Study Report No. 53.
26. Tong, Wen-How, Schumacker, Cornell, C.A., Whitman, R.V. (1975) "Seismic Hazard Maps for Massachusetts," M.I.T. Internal Study Report No. 52.
27. Whitman, R.V. Unpublished notes.
28. Whitman, R.V. et al "Methodology and Pilot Application" M.I.T. Civil Engineering Dept. Report R74-15.

Appendix A

Derivation of the probability of exceedance for one point source and one site:

- (I) Magnitude-frequency law: for a linear magnitude-frequency law with upper bound m_1 and lower bound m_0 , the following equation applies:

$$\log n(m) = \begin{cases} 0 & m \leq m_0 \\ a - b(m - m_0) & m_0 \leq m \leq m_1 \\ 0 & m \geq m_1 \end{cases} \quad (A1)$$

This implies that the cumulative distribution of magnitude to have following forms:

$$\begin{aligned} \text{(i) } m_0 \geq m & \quad F_M(m) = 0 \\ \text{(ii) } m_0 \leq m \leq m_1 & \quad F_M(m) = k_{m_1} (1 - e^{-\beta(m - m_0)}) \\ \text{(iii) } m \geq m_1 & \quad F_M(m) = 1 \end{aligned} \quad (A2)$$

- (II) Attenuation law: as suggested by Cornell the probabilistic attenuation law has the form

$$Y = b_1 e^{b_2 M} R^{-b_3} \varepsilon \quad (A3)$$

where $\ln \varepsilon$ is normally distributed with mean zero and standard deviation σ

(III) For a given point source and a given value of $\ln \xi$, the risk that the site ground acceleration will exceed level y can be stated as:

$$\begin{aligned} & P(Y \geq y | \text{earthquake } i; \ln \xi) \\ &= P(b_1 e^{b_2 M} R^{-b_3} \xi \geq y | \text{earthquake } i; \ln \xi) \\ &= P\left(M \geq \frac{1}{b_2} \ln \frac{R^{b_3} y}{b_1} - \frac{\ln \xi}{b_2} \mid \text{earthquake } i; \ln \xi\right) \quad (\text{A4}) \end{aligned}$$

To find $P(Y \geq y | \text{Earthquake } i)$ we have to integrate through all positive and negative values of $\ln \xi$, thus:

$$P(Y \geq y | \text{earthquake } i) = \int_{-\infty}^{+\infty} P(Y \geq y | \text{earthquake } i; \ln \xi) f_{\ln \xi}(\ln \xi) d \ln \xi \quad (\text{A5})$$

where $f_{\ln \xi}(\ln \xi)$ is the probability density function of $\ln \xi$

$$f_{\ln \xi}(\ln \xi) = \frac{1}{\sigma_{\ln \xi} / \sqrt{2\pi}} \left[-\frac{1}{2} \exp\left(-\frac{\ln \xi}{\sigma_{\ln \xi}}\right)^2 \right] \quad (\text{A6})$$

Let's call $\ln \xi = x$ for notational convenience.

$$P(Y \geq y | \text{earthquake } i) = \int_{-\infty}^{+\infty} P\left(M \geq \frac{1}{b_2} \ln \frac{R^{b_3} y}{b_1} - \frac{x}{b_2} \mid \text{quake } i; \ln \xi\right) f_X(x) dx \quad (\text{A7})$$

The limit of integration $(-\infty, +\infty)$ of x has to be broken into 3 ranges so that correct form of $F_M(m)$ is adopted within each range.

$$(i) \frac{1}{b_2} \ln \frac{R^{b_3} y}{b_1} - \frac{x}{b_2} \leq m_0 \longrightarrow \bar{F}_M(m) = 0$$

$$x \geq z_2 \quad (A8)$$

$$\text{where } z_2 = \ln y - \ln(b_1 e^{b_2 m_0} R^{-b_3})$$

$$(ii) m_0 \leq \frac{1}{b_2} \ln \frac{R^{b_3} y}{b_1} - \frac{x}{b_2} \leq m_1 \longrightarrow \bar{F}_M(m) = k_{m_1} (1 - e^{-\beta(m-m_0)})$$

$$z_2 \geq x \geq z_1 \quad (A9)$$

$$\text{where } z_1 = \ln y - \ln(b_1 e^{b_2 m_1} R^{-b_3})$$

$$(iii) \frac{1}{b_2} \ln \frac{R^{b_3} y}{b_1} - \frac{x}{b_2} \geq m_1 \longrightarrow \bar{F}_M(m) = 1$$

$$x \leq z_1 \quad (A10)$$

$$\text{Thus } P\{Y \geq y | \text{quake } i\} = \int_{-\infty}^{+\infty} P\{M \geq \frac{1}{b_2} \ln \frac{R^{b_3} y}{b_1} - \frac{x}{b_2} | \text{quake } i\} f_X(x) dx$$

$$= \int_{-\infty}^{z_1} [1 - \bar{F}_M(\frac{1}{b_2} \ln \frac{R^{b_3} y}{b_1} - \frac{x}{b_2})] f_X(x) dx + \int_{z_1}^{z_2} [1 - \bar{F}_M(\frac{1}{b_2} \ln \frac{R^{b_3} y}{b_1} - \frac{x}{b_2})] f_X(x) dx$$

$$+ \int_{z_2}^{+\infty} [1 - \bar{F}_M(\frac{1}{b_2} \ln \frac{R^{b_3} y}{b_1} - \frac{x}{b_2})] f_X(x) dx$$

$$= \int_{z_1}^{z_2} f_X(x) dx - \int_{z_1}^{z_2} k_{m_1} [1 - e^{-\beta(\frac{1}{b_2} \ln \frac{R^{b_3} y}{b_1} - \frac{x}{b_2} - m_0)}] f_X(x) dx + \Phi^*(z_2/\sigma)$$

where $\Phi^*(\cdot)$ is the cumulative distribution function of

standardized Gaussian distribution $\Phi^*\left(\frac{Z_1}{\sigma}\right) = \frac{1}{\sqrt{2\pi}} \int_{\frac{Z_1}{\sigma}}^{\infty} e^{-\frac{1}{2}x^2} dx$.

$$\begin{aligned} P(Y \geq y | \text{quake } i) &= \Phi^*\left(\frac{Z_1}{\sigma}\right) - k_{m_1} [\Phi^*\left(\frac{Z_1}{\sigma}\right) - \Phi^*\left(\frac{Z_2}{\sigma}\right)] + \int_{Z_1}^{Z_2} e^{\beta m_0} R^{-\frac{b_3 \beta}{b_2} \left(\frac{y}{b_1}\right) - \frac{\beta}{b_2} x} e^{-\frac{\beta x}{b_2}} f_X(x) dx \\ &= k_{m_1} \Phi^*\left(\frac{Z_2}{\sigma}\right) + (1 - k_{m_1}) \Phi^*\left(\frac{Z_1}{\sigma}\right) + k_{m_1} e^{\beta m_0} R^{-\frac{b_3 \beta}{b_2} \left(\frac{y}{b_1}\right) - \frac{\beta}{b_2} x} \int_{Z_1}^{Z_2} e^{-\frac{\beta x}{b_2}} f_X(x) dx \end{aligned} \quad (A11)$$

$$\begin{aligned} \text{where } \int_{Z_1}^{Z_2} e^{-\frac{\beta}{b_2} x} f_X(x) dx &= \int_{Z_1}^{Z_2} e^{-\frac{\beta}{b_2} x} \frac{1}{\sigma \sqrt{2\pi}} e^{-\frac{1}{2} \left(\frac{x}{\sigma}\right)^2} dx \\ &= \int_{Z_1}^{Z_2} \frac{1}{\sigma \sqrt{2\pi}} e^{-\frac{\beta}{b_2} x - \frac{1}{2} \frac{x^2}{\sigma^2}} dx \\ &= e^{-\frac{\beta^2 \sigma^2}{2b_2^2}} \int_{Z_1}^{Z_2} \frac{1}{\sigma \sqrt{2\pi}} \exp\left[-\frac{1}{2} \left(\frac{x - \frac{\beta \sigma^2}{b_2}}{\sigma}\right)^2\right] dx \\ &= e^{-\frac{\beta^2 \sigma^2}{2b_2^2}} \left[\Phi^*\left(\frac{Z_1}{\sigma} - \frac{\beta \sigma}{b_2}\right) - \Phi^*\left(\frac{Z_2}{\sigma} - \frac{\beta \sigma}{b_2}\right) \right] \end{aligned}$$

So the final result is :

$$\begin{aligned} P(Y \geq y | \text{quake } i) &= k_{m_1} \Phi^*\left(\frac{Z_2}{\sigma}\right) + (1 - k_{m_1}) \Phi^*\left(\frac{Z_1}{\sigma}\right) + k_{m_1} \left[\Phi^*\left(\frac{Z_1}{\sigma} - \frac{\beta \sigma}{b_2}\right) - \Phi^*\left(\frac{Z_2}{\sigma} - \frac{\beta \sigma}{b_2}\right) \right] \times \\ &\quad e^{-\frac{\beta^2 \sigma^2}{2b_2^2}} e^{\beta m_0} R^{-\frac{b_3 \beta}{b_2} \left(\frac{y}{b_1}\right) - \frac{\beta}{b_2} x} \end{aligned} \quad (A12)$$

Appendix B

List of Figures	<u>Page</u>
Figure 1 Seismic Risk Curve	51
Figure 2 Seismic Risk Map for 1000 Yr. Return Period	52
Figure 3 Mean Yearly Number of Earthquakes of Magnitude Greater Than M for Different Regions	53
Figure 4 Frequency Magnitude Relationship	54
Figure 5 Least Squares to Peak Ground Accelerations	55
Figure 6 Source-Site Geometry	56
Figure 7 Spatially Distributed System	56
Figure 8 Modeling of Uniform Source Area	57
Figure 9 Risk Curve of Two Site Case	58
Figure 10 Risk Curve of Two-Site Case	59
Figure 11 Risk Curve of Two-Site Case	60
Figure 12 General Source-Site Geometry	61
Figure 13 Normalized Risk Curve	62
Figure 14 Sensitivity Study	63
Figure 15 Sensitivity Study	64
Figure 16 Normalized Risk Curve	65
Figure 17 Sensitivity Study	66
Figure 18 Sensitivity Study	67

		<u>Page</u>
Figure 19	Normalized Risk Curve	68
Figure 20	Risk Curve	69
Figure 21	Risk Curve	70
Figure 22	Risk Curve	71
Figure 23	Seismic Risk Curve of Two-Site Case	72
Figure 24	Seismic Risk Curve of Two-Site Case	73
Figure 25	Cost Benefit Analysis	74

Appendix C

List of TablesPage

Table 1	Conversion Table of β	14
Table 2	Stability Study	75
Table 3	Stability Study	75
Table 4	Stability Study	76
Table 5	Stability Study	76
Table 6	Stability Study	77
Table 7	Stability Study	77

